Marine Geology 443 (2022) 106648

Contents lists available at ScienceDirect

Marine Geology

journal homepage: www.elsevier.com/locate/margo

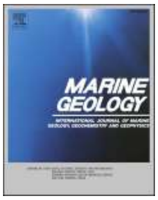

Research Paper

A multiproxy reconstruction of the Late Pleistocene-Holocene paleoenvironment: New insights from the NW Black Sea

Gabriel Ion [a], Andrei Briceag [a], Dan Vasiliu [b], Naliana Lupaşcu [b], Mihaela Melinte-Dobrinescu [a,*]

[a] *Institute of Marine Geology and Geo-ecology, 23-25 Dimitrie Onciul, RO-024053 Bucharest, Romania*
[b] *Institute of Marine Geology and Geo-ecology, 304 Mamaia Blv., RO-900581 Constanța, Romania*

ARTICLE INFO

Editor: Shu Gao

Keywords:
Paleoenvironment
Red-brownish sediments
Calcareous nannoplankton
Ostracods
Geochemistry

ABSTRACT

We provide new data on the Black Sea evolution during the preconnection and reconnection stages with the Mediterranean, based on sedimentology, geochemistry, calcareous nannoplankton and ostracods analysis, in 13 cores placed between 141 m and 1315 m water depths. Unit 1 – The Coccolith Mud, Unit 2 - The Sapropel Mud and Unit 3 – The Lacustrine Lutite, including red-brownish depositional intervals, were identified in all studied deep-water cores. These units are not present in a shallow setting, i.e., above 166.7 m water depth, being replaced by sandy levels and shell debris. The red-brownish layers are interpreted as hyperpycnites, but some of the red successions show turbidite features, especially the ones situated on canyon sides, at a water depth below 600 m. In the oldest intercepted Unit 3 of the Neoeuxinian lake, $CaCO_3$ values are constantly low, but towards the top of this unit they show two distinct peaks, interpreted as signals of Bølling–Allerød and Preboreal interstadials. In between, a significant decrease in $CaCO_3$ values, linked to the setting of the Younger Dryas, is coincident in the deep cores with diatom blooms and high frequency of ostracods related to cooler waters. The scarce but continuous occurrence of *Emiliania huxleyi* nannoplankton species from the top of Unit 3 indicates that the salinity was at least 10–11‰ prior the Sapropel Mud deposition and increase at a least 17‰ within the lower part of Unit. 2. In the same interval, the Ponto-Caspian ostracods are still present. The Mediterranean ostracods consistently occur from the top of Unit 2, when bottom water salinity reached values for allowing their survival. The first bloom of *E. huxleyi* is placed at the base of Unit 2, where coccolith laminae occur, while the second bloom is placed in Unit 1 that contains exclusively Mediterranean ostracods and consistent assemblages of benthonic foraminifers, similar with the ones present today.

1. Introduction

The Black Sea is a very peculiar basin, due to its character of a semi-enclosed sea and its episodic connectivity with the world ocean via the Mediterranean and with the Caspian Sea during the Pleistocene-Quaternary interval. This peculiarity produced a complex pattern of paleoshorelines and paleohydrography, imprinted in the sedimentary structures deposited and/or eroded, on the actual continental platform and in the shelf break area. The sea level fluctuations have been convoluted with other local, regional or global phenomena, such as differential compaction of the young sediments, regional active tectonics and glacial isostatic adjustment.

During the Last Glacial Maximum (LGM), 25,000–18,000 y BP (years Before Present), a stable and cooler climate mode was hypothesized (Major et al., 2002, 2006; Bahr et al., 2005). Within Heinrich Stadial 1 (HS-1), between 18,000–14,700 y BP, the first Fennoscandian Meltwater Pulse in the Black Sea occurred, which produced a high deglacial sedimentary input (Major et al., 2002; Bahr et al., 2005; Soulet et al., 2013). Previous studies (Chepalyga, 1984; Chepalyga et al., 2004; Major et al., 2006; Yanko-Hombach and Kislov, 2018) indicate that, during the HS-1, the Caspian Sea spillover into the Black Sea through the Manych Corridor; this event was coincident with the delivery of huge amount of water and sediment brought by the Volga River, following the meltwater.

The interval encompassing the Late Pleistocene to Holocene provokes a special interest of the scientific community, particularly due to the reconnection of the Black Sea with Mediterranean via the Bosphorus Strait, event supposed to remain in the collective memory as the Biblical

---

* Corresponding author.

E-mail addresses: gion@geoecomar.ro (G. Ion), andrei.briceag@geoecomar.ro (A. Briceag), dan.vasiliu@geoecomar.ro (D. Vasiliu), naliana.lupascu@geoecomar.ro (N. Lupaşcu), melinte@geoecomar.ro (M. Melinte-Dobrinescu).

https://doi.org/10.1016/j.margeo.2021.106648
Received 19 March 2021; Received in revised form 15 September 2021; Accepted 18 September 2021

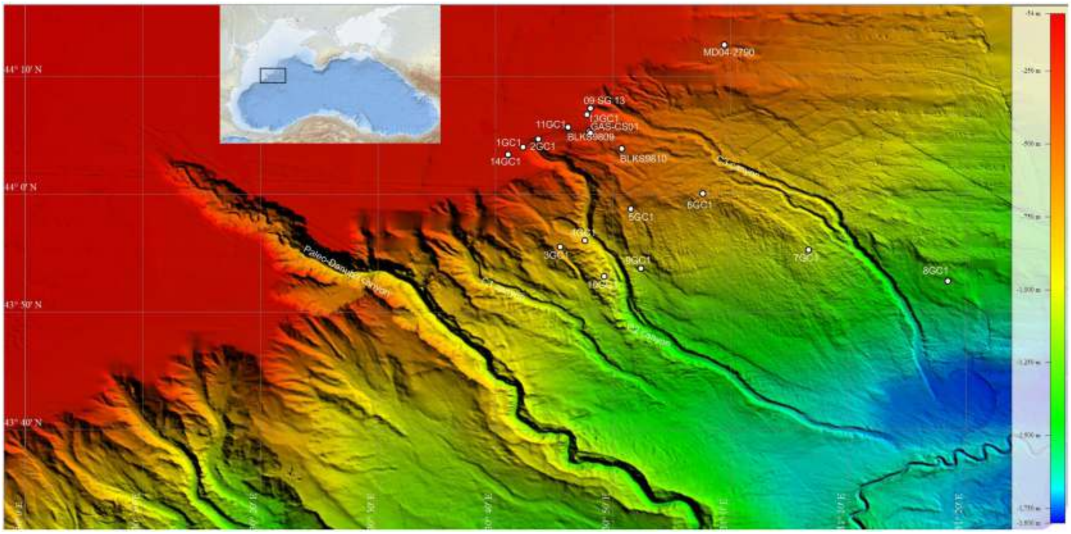

Fig. 1. Location in the NW Black Sea of the 13 investigated gravity cores (1gs to 14 GC). Bathymetry data from https://tiles.emodnet-bathymetry.eu/preview.html and the National Institute of Marine Geology and Geo-ecology (GeoEcoMar). Location of the cores MD04-–2790 after Giunta et al. (2007), BLKS9809, BLKS9810 from Major et al. (2002), 09 SG 13 after Briceag et al. (2019) and Core GAS CS 01 after Martinez-Lamas et al. (2020).

Table 1
Location and length of the investigated gravity cores.

No.	Core	Water depth (m)	Latitude	Longitude	Length (cm)
1	1GC1	172	44.066905	30.705683	424
2	2GC1	166.7	44.078077	30.727152	266
3	3GC1	655.7	43.925442	30.757762	401
4	4GC1	840.3	43.934597	30.792775	379
5	5GC1	620	43.979324	30.858259	413
6	6GC1	648.5	44.00088	30.959473	415
7	7GC1	1053	43.921896	31.10902	442
8	8GC1	1315	43.87697	31.306242	376.5
9	9GC1	1027	43.894939	30.872039	372
10	10GC1	940.1	43.883458	30.820202	430
11	11GC1	160.9	44.095323	30.768806	364
12	13GC1	171.4	44.112776	30.795611	347
13	14GC1	141.1	44.056592	30.68407	186

Table 2
Weight of the micropaleontological samples from 1GC1 gravity core.

No.	Sample interval (cm)	Weight (grams)
1	0–5	20.4170
2	5–10	20.7860
3	10–15	22.5337
4	15–21	58.2080
5	21–26	137.22
6	26–30	110.3665
7	30–35	120.55
8	35–40	125.7045
9	55–60	130.82
10	90–95	112.0495
11	120–125	112.0856
12	140–145	114.46
13	145–149	103.6034
14	149–153	81.6590
15	153–158	122.3876
16	184–189	109.0512
17	220–225	145.3615
18	270–275	146.3938
19	355–360	179.20
20	420–424	157.3529

Table 3
Weight of the micropaleontological samples from 3GC1 gravity core.

No.	Sample interval (cm)	Weight (grams)
1	0–3	20.72
2	3–6	17.49
3	6–9	19.07
4	9–12	22.30
5	12–15	17.64
6	15–18	18.23
7	18–21	19.73
8	21–24	20.66
9	30–33	14.24
10	33–36	11.56
11	36–39	10.23
12	45–48	15.00
13	48–53	59.98
14	53–58	75.64
15	95–100	73.51
16	155–160	83.54
17	185–190	84.56
18	200–205	77.96
19	230–235	78.22
20	235–240	76.17
21	285–290	89.43
22	348–353	87.83
23	370–375	89.27
24	396–401	81.51

Noah's Flood (Ryan et al., 1997, 2003). There are three main scenarios regarding the way of reconnection between the Black Sea and Mediterranean, topic of an intense and ongoing debate in the scientific community. Ryan et al. (1997) proposed a catastrophic flood that took place at a rate approaching tens of cm per day, assuming that the sea-level of the Mediterranean had a significant rapid rising. By contrast, some authors (i.e., Aksu et al., 1999, 2002; Hiscott and Aksu, 2002; Hiscott et al., 2007; Kaminski et al., 2002) believed that there was no rapid entry of salt water during reconnection between the two marine basins. Hence, an outflow of the Black Sea waters through the Bosphorus Strait in the Mediterranean took place at around 11.900 y BP; later, between 8500 and 8000 y BP, the two-way water circulation between the Black Sea and the Mediterranean established through the Bosphorus Strait (Marret et al., 2009). A third scenario emphasized that the reconnection between the two marine basins was not in one step, neither rapid, but in an oscillatory regime during thousands of years (Yanko-Hombach, 2007; Yanko-Hombach et al., 2014). Some authors (Nicholas et al., 2011) assume a rapid Holocene sea-level rise in the Black Sea, i.e., a prompt transgression in 400 years, but a gradual salinity increase at

Table 4
Weight of the micropaleontological samples from 8GC1 gravity core.

No.	Sample interval (cm)	Weight (grams)
1	0–3	23.79128
2	3–6	19.4320
3	6–9	22.8264
4	9–14.5	22.4992
5	14.5–20	15.5871
6	20–25	12.2328
7	30–35	5.6055
8	35–38	6.8179
9	38–43	48.7339
10	43–48	56.7685
11	48–53	22.3732
12	85–90	46.0444
13	90–95	48.8952
14	95–100	41.5337
15	100–105	38.0104
16	110–115	35.9802
17	122–127	47.6896
18	127–132	43.2440
19	132–137	45.1497
20	170–172	44.5633
21	213–218	44.5732
22	230–235	44.4278
23	235–240	57.4719
24	290–295	55.2444
25	317–322	47.9628
26	322–328	26.7398
27	365–370	42.0006

around 1000 years.

The timing of the flooding event is also a matter of debate. Based on microfaunal assemblages some authors, i.e., Ryan et al. (1997), supposed a rapid flood event at 7100 y BP, based on dated shells from sediment cores. Soulet et al. (2011) assumed, based on analyzed microfossils, a first occurrence of the marine species at 9000 y BP, while Yanko-Hombach et al. (2014) indicated that the marine species appeared in the Black Sea gradually, after 8900 y BP. The study of the macro- and microfossils in NW Black Sea cores, corroborated with absolute ages, shows that the reconnection of the Black Sea with the Mediterranean took place at 9380 y BP (Briceag et al., 2019). Older ages for the reconnection were assumed by Aksu et al. (2002) and Major et al. (2002) at 12,800 y BP, based on lithostratigraphic and seismic investigation.

Recently, Riboulot et al. (2018) hypothesized that the long-term isolation of the Black Sea basin, followed by the reconnection with the Mediterranean, produced significant water salinity fluctuation, along with diffusion into the sediment; thus, the sediment pore water salinity was substantially modified. The aforementioned authors assume that these processes were the driving force behind the dissociation of gas hydrates over large areas of the Black Sea.

Goldberg et al. (2016) presented various scenarios concerning sea-level change since LGM in the Straits of Bosphorus and Dardanelles regions, based on geophysical data; glacial isostatic modifications were also taken into account. They pointed out that a reconnection of Mediterranean with the Black Sea at around 9000 y. BP led to a lowering of the Bosphorus Sill through erosion by 14–21 m during and after the flood. On the other hand, if the flood took place at around 7000 y. BP, the sill erosion might be more pronounced, about 24–31 m since the flood event, value which is hard to imagine.

Some scientists hypothesized that the water level of the Black Sea was, during LGM, between 80 and 100 m below the present-day one, while the basin had totally a freshwater character (Fedorov, 1978; Yanko, 1990; Ryan et al., 1997; Popescu et al., 2001; Lericolais et al., 2013). In the NW Black Sea shore region, i.e., Danube Delta, the paleogeomorphology along with lithological changes and radiocarbon analysis (Giosan et al., 2009) led to the conclusion that the Black Sea level before LGM was not so low, only around 30 m below present-day. Soulet et al. (2011, 2013) mentioned, based on ^{14}C radiocarbon reservoir age, that only at the end of the Black Sea Meltwater Pulses, the water level was around 30 m below the present day one, while a high sea level occurred probably during the Bølling–Allerød warm interval (Lericolais et al., 2010). The aforementioned authors point out that after the Younger Dryas cold period, the water level dropped again to around -100 m.

During LGM, the Black Sea was most probably a low salinity landlocked lake, i.e., <8–10‰ of surface waters (Hiscott and Aksu, 2002; Yanko-Hombach, 2007; Marret et al., 2009; Mertens et al., 2012). Evidence for fresh to brackish Black Sea water existence during the regional Neoeuxine stratigraphic interval (Nevesskaya, 1965), comprising the glacial and deglacial interval up to the reconnection with the Mediterranean, comes from fluctuation shown by various groups of organisms, such as foraminifers, ostracods, calcareous nannofossils, diatoms, dinoflagellates and mollusks, along with pore-water chemistry and isotope fluctuation (Ross et al., 1970; Bukry, 1974; Giunta et al., 2007; Soulet et al., 2010; Oaie and Melinte-Dobrinescu, 2012; Mudie et al., 2014; Yanko-Hombach et al., 2014; Williams et al., 2018; Briceag et al., 2019, among many others). Based on porewater analysis, Soulet et al. (2010) and Ruffine et al. (2021) assumed that the glacial Black Sea was a homogeneous freshwater lake with a chlorine content of <2‰. Yet, some published data are contradictory; a scenario of a gradual increase of the salinity has been advanced, or by contrast an abrupt salinity rise has been supposed. Concerning the regional climate, it was suggested that, around the boundary between Bølling–Allerød and Younger Dryas, the climate was leading the interannual variability in the run-off of the Danube; this feature might reflect the climate mode of the whole central Europe (Bahr et al., 2006; Sanchi et al., 2014).

The aim of this study is to refine the Romanian Black Sea paleosetting for the last, Upper Pleistocene-Holocene interval based on integration of lithological data, fossil record (i.e., microfaunas and calcareous algae) and geochemistry. New data on the red-brownish clays deposition during the LGM, along with paleoenvironmental and paleoecological reconstructions, are also presented herein.

2. Regional setting

The present-day Black Sea basin is bordered by the Pontic Mountains to the south, the Caucasus and Crimea Mountains to the east, northeast and north respectively, and the low land of the Dobrogea region with the Danube Delta to the north and west. The Danube, Dnieper, Dniester and Southern Bug rivers flow into the northwestern and northern Black Sea and discharge a significant sedimentary and water input (Tolmazin, 1985; Panin and Jipa, 2002; Hiscott et al., 2007). The NW shelf is the largest one in the Black Sea, representing 30% of the basin (Goncharov, 1958). Thus, the NW part of the Black Sea has the widest shelf area of the present-day basin, with the outer limit varying between 140 and 180 m water depth. This spatial development is both an advantage in studying the Pleistocene-Holocene evolution, but also a disadvantage, because of the complexity of the morphological patterns and sub-bottom structures; these features are linked to the paleoshorelines migration and/or erosion, along with the incision, filling up and erosion of paleo-valleys, which developed on the emerged continental platform of glacial times.

Another very important feature of NW Black Sea is a large deep-sea fan complex, the Danube Deep-Sea Fan, which extends about 150 km down slope (Popescu et al., 2001; Lericolais et al., 2013). The Danube Deep-Sea Fan complex hosts accumulations of methane hydrates and peculiar four stacked Bottom Simulating Reflections (BSRs) feature; that quite strange cluster of BSRs could be the result of the vertical migration of the gas hydrates stability zone, in response to the Quaternary sea-level variation (Ion et al., 2002).

Ross and Degens (1974) were the first to describe the detailed Upper Pleistocene-Holocene lithostratigraphy of the Black Sea. They identified on the slope and deep parts of the Black Sea, below 200 m water depth, several lithological units that are still in use (from younger to older): (i)

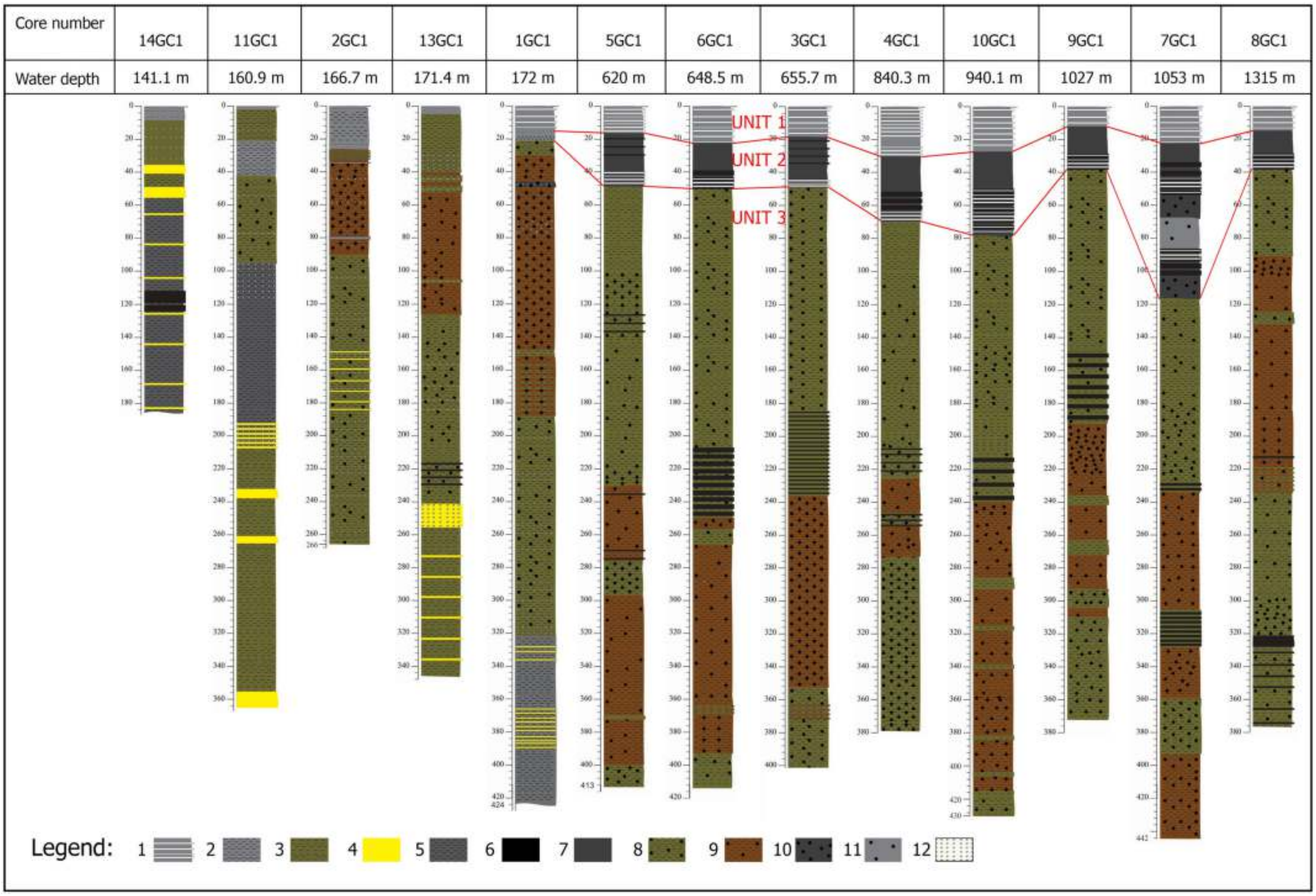

Fig. 2. Lithology of the investigated gravity cores. Legend: 1 - light gray mud with coccolith laminae; 2 – light gray mud; 3 - Gy-greenish silty clays; 4 - fine silty sands; 5 - dark gray clays; 6 - black organic matter; 7 - sapropel muds; 8 - Gy-greenish silty clays with specks of black organic matter; 9 - reddish-brown clays with specks of black organic matter; 10 - sapropel mud with specks of black organic matter; 11 - light gray mud with specks of black organic matter; 12 - coquina layer. UNIT 1 - The Coccolith Mud, UNIT 2 - The Sapropel Mud and UNIT 3 - The Lacustrine Lutite. (For interpretation of the references to colour in this figure legend, the reader is referred to the web version of this article.)

The Coccolith- Mud “Unit 1”; (ii) the Sapropel Muds “Unit 2”, and (iii) The Neoeuxinic Muds “Unit 3”, also described as the Lacustrine Lutite. This lithostratigraphy was confirmed by all the investigations carried out since the 1970s, including the ones developed in the frame of the European Projects EROS, Blason and Assemblage, between the years 1998 and 2005 (Lericolais et al., 2006; Popescu et al., 2006; Strechie-Sliwinski, 2007). Bukry et al. (1970), 1974) found both calcareous nannoplankton species *Emiliania huxleyi* and *Braarudosphaera bigelowii* in Unit 1, where the salinity was above 17‰ for allowing their survival; the authors proposed that the fine laminae <1 mm in thickness might represent annual blooms of *E. huxleyi*.

A lithologic feature of Unit 3 described by Ross and Degens (1974) is the occurrence of red-brownish clays, interbedded with gray-greenish ones, in the cores of the western Black Sea (Ryan, 2007). Recent studies (Soulet et al., 2013) linked their origin to two possible provenances: (i) drainage of the Fennoscandian ice sheet through the Dnieper River, via proglacial Lake Disna into the Black Sea, or (ii) through the Danube River, supplied by glaciers from the Alps. Ryan et al. (2013) summarized data from 30 cores located in the Western part of the Black Sea and identified the red-brownish deposition in all of them. The authors did not identify them in the eastern Black Sea region.

In a shallow setting of NW Black Sea, the Late Pleistocene to Holocene Units 1, 2 and 3 of Ross and Degens (1974) are not recognizable. Instead, during the aforementioned interval, the “Shallow Unit” (Giunta et al., 2007) was deposited. This unit overlies a ‘shell hash’ depositional interval with coquina levels and a structureless gray yellowish clay devoided of Holocene calcareous nannoplankton taxa (Oaie and Melinte-Dobrinescu, 2012).

Concerning the microfaunas, in the NW Black Sea, only few benthonic foraminifers that survive at high salinity fluctuations, such as *Ammonia beccarii* and *Elphidium* spp., are present. *Ammonia* species live in normal marine to lagoonal environments with a salinity ranging from 32 to 65‰ (Reinhardt et al., 1994). The species of *Ammonia* and *Elphidium* genera could be found also in a very shallow marine setting, i.e., in the NW Black Sea, in front of the Danube Delta (Mudie and Yanko-Hombach, 2019), where salinity is between 5 and 8‰. The ostracods show a distinct distribution pattern, being Ponto-Caspian in origin within the Pleistocene and mainly Mediterranean in the Holocene (Stancheva, 1989; Boomer et al., 2003; Yanko-Hombach, 2004; Soulet et al., 2010; Briceag et al., 2019, among many others).

3. Material and methods

A number of 13 gravity cores, located in the NW Black Sea (Fig. 1 and Table 1) have been studied. All cores have been described in detail from lithological/sedimentological point of view and sampled for multiproxy analyses. The core length is between 184 cm and 442 cm. The cores were acquired in September 2018 during a scientific cruise performed with the GeoEcoMar R/V *Mare Nigrum*.

To perform micropaleontological studies, a total of 91 micropaleontological samples (20 samples from core 1GC1, 36 samples from core 3GC1 and 35 samples from core 8GC1) have been processed, boiled with

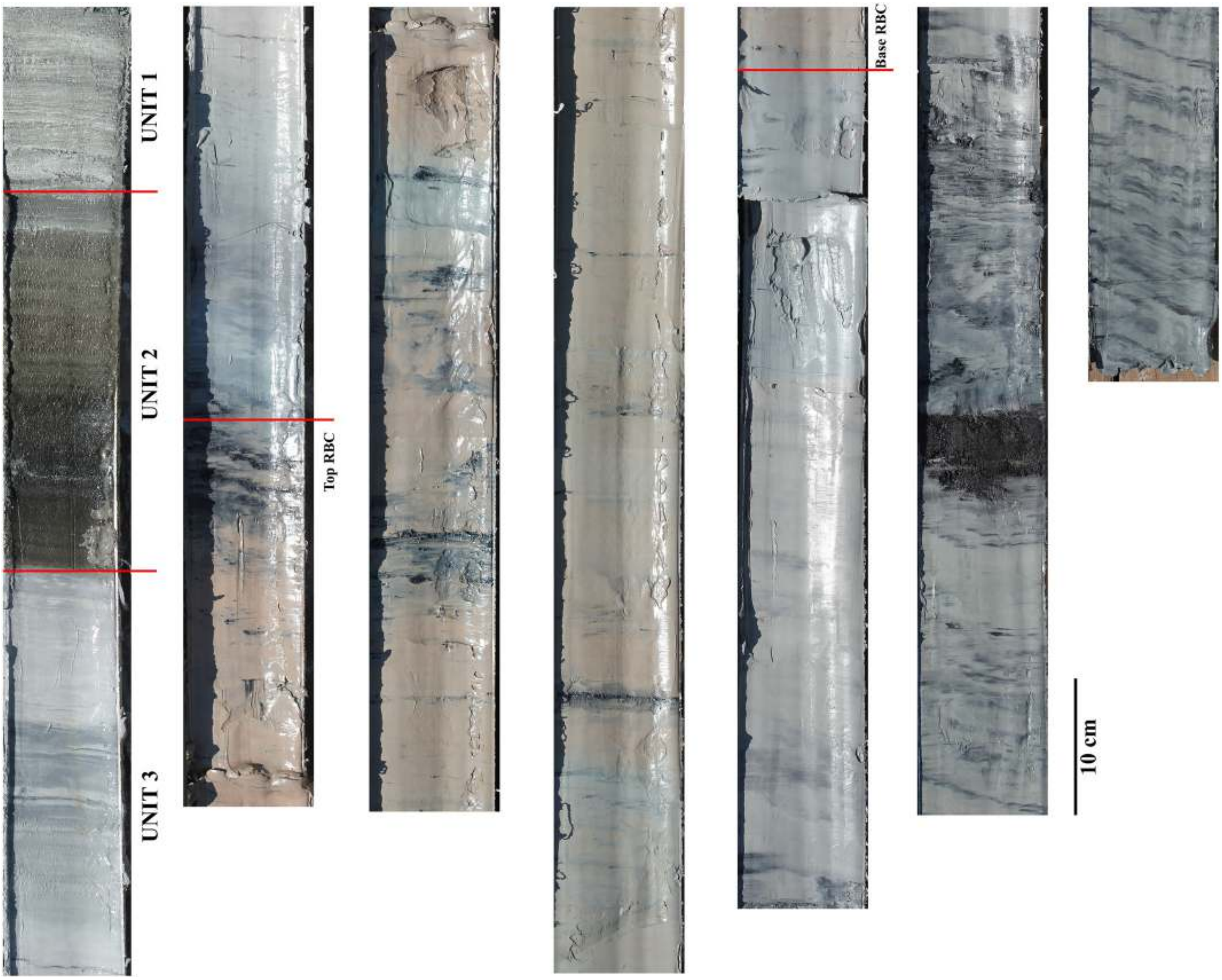

Fig. 3. Photographs of the Core 8GC1 (location in Fig. 1) showing the main lithological units encountered at the 172 m water depth; youngest sediments to the left; the first 10 cm represent youngest UNIT 1 (The Coccolith Mud), which follows UNIT 2 (The Coccolith Mud) and UNIT 3 (The Lacustrine Lutite) to the base of the core.

Na_2CO_3, washed through a 63 μm sieve, air-dried and hand-picked under an Olympus binocular microscope. To take photographs of the microfaunal taxa we used a Canon 550D camera mounted on the microscope. Ostracod and foraminiferal assemblages were investigated for their diversity and abundance. Quantitative studies were achieved for both ostracods and foraminifers by counting the total number of specimens. The micropaleontological sediment samples were dried and weighed (Tables 2–4). The weight of the samples varies between 5.6 and 157 g. For quantitative analyses of ostracods, we have considered only adult specimens (whole adult valves and carapaces specimens of each sample were counted, carapaces being counted as one specimen).

Due to the possibility of successive molt of taxa, juvenile specimens were not taken into account for the relative abundance. The ostracod juvenile and adult specimens were considered separately for the differentiation between in situ and transported taxa (as used by Boomer et al., 2003). For the qualitative studies, we followed the abundance and diversity fluctuation pattern of the microfossil assemblages, along with the ecological affinities of each species, such as salinity and temperature. Reference materials used for identification follow Schornikov (1964, 2011), Olteanu (1978), Stancheva (1989), Boomer et al. (2003, 2010), Ivanova et al. (2007), Opreanu (2008) and Zenina et al. (2017).

The calcareous nannofossil content of 217 samples has been analyzed, in the same cores studied for the microfaunal content, i.e., 1GC1, 3GC1 and 8GC1. The samples have been taken each 3 cm for the Units 1 and 2 and 5 cm for the Unit 3; we have sampled at larger intervals, i.e., 10 cm, within the red clays. Qualitative and quantitative investigations have been carried out by using an Olympus LM (light microscope), with 1600× magnification. The qualitative investigations have been made by counting the nannofossils in a fixed area that corresponds to 75.5 fields. The counts were converted into population density (number/mm^2), as used by Giunta et al. (2007). Results concerning the nannofossils of the core 3GC1 were previously published in Melinte-Dobrinescu et al. (2019). Diatoms were identified in some samples prepared for the calcareous nannoplankton analysis; no specific analysis on the diatoms have been performed.

The $CaCO_3$ has been computed based on the CO_2 concentration, as volumetric test, which consists of titration with HCl 0.5 N of a measured sediment quantity and has been measured by retro titration with NaOH 0.5 N, in the presence of phenolphthalein, in excess of the acid. The total organic carbon (TOC) has been analyzed by titration, based on the oxidation of carbon with excess of potassium dichromate, in sulfuric acid medium and retrotitration of the excess of the dichromate with

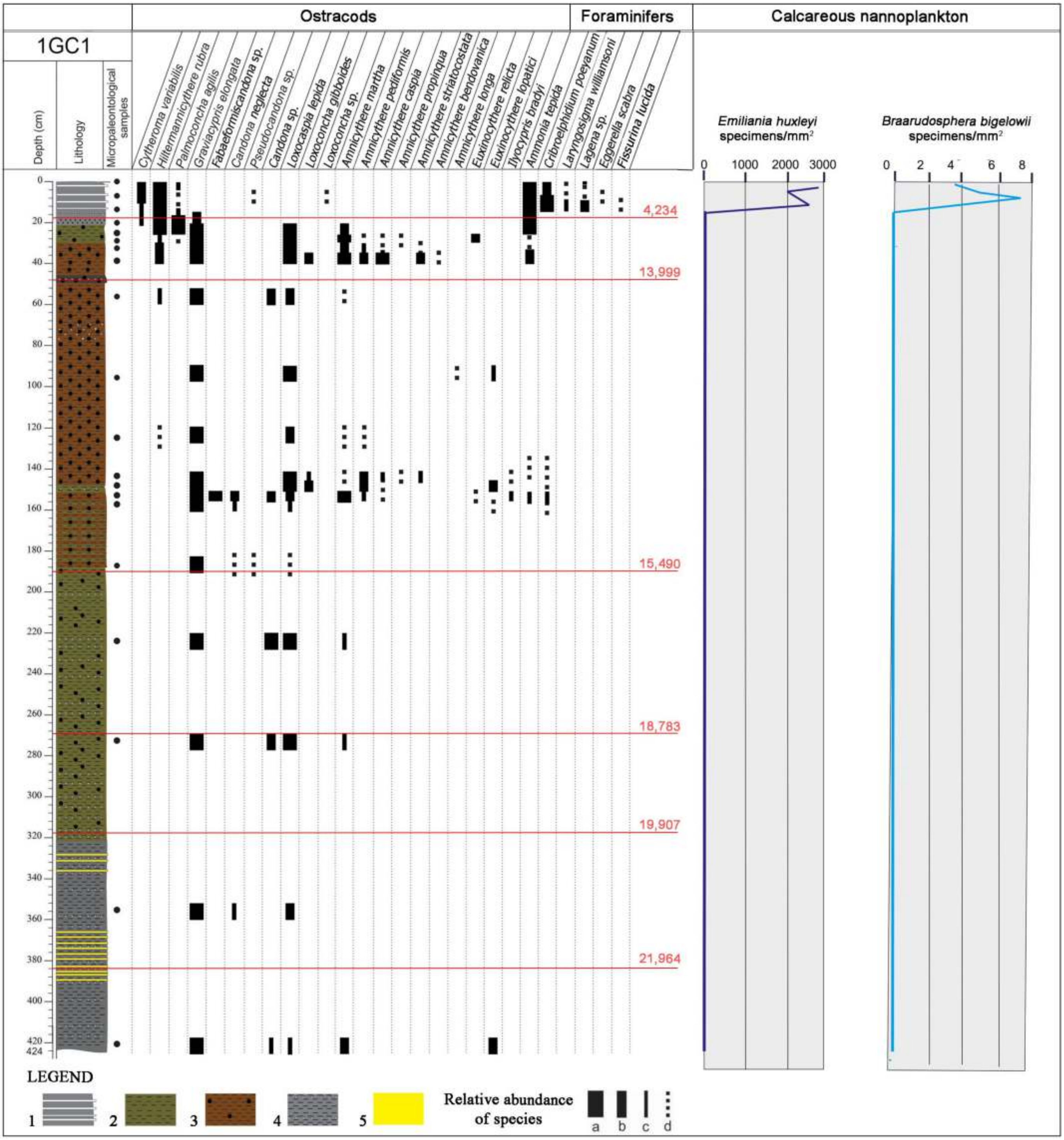

Fig. 4. Microfaunal (ostracods and foraminifers) distribution and abundance and fluctuation in abundance of calcareous nannoplankton taxa *Emiliania huxleyi* and *Braarudosphaera bigelowii* (specimens/mm^2) in Core 1GC1. Relative abundance of ostracods and foraminifers: a: ≥ 20 specimens; b: 7–20 specimens; c: 4–6 specimens; d: 1–3 specimens. Absolute ages after Nagavciuc et al. (2021). For lithology see legend in Fig. 2.

Mohr salt in the presence of diphenylamine as indicator, following the methodology of Gaudette et al. (1974).

The total organic matter (TOM) has been determined by comparing the mass of sediment before and after calcination. The sample, previously dewatered at 105 °C/24 h, to determine the sediment moisture, is calcinated at least 16 h at 375 °C and the cooled residue is then weighted. The difference between the two weights, divided by the initial mass of the sediment sample was calculated as TOM.

4. Results

4.1. Lithology

In 8 cores from the total of 13 investigated, a complete record of the three Upper Pleistocene-Holocene lithological units of Ross and Degens (1974) has been identified. This lithology was observed between 620 and 1315 m water depths (Fig. 2) and it is characterized by the following

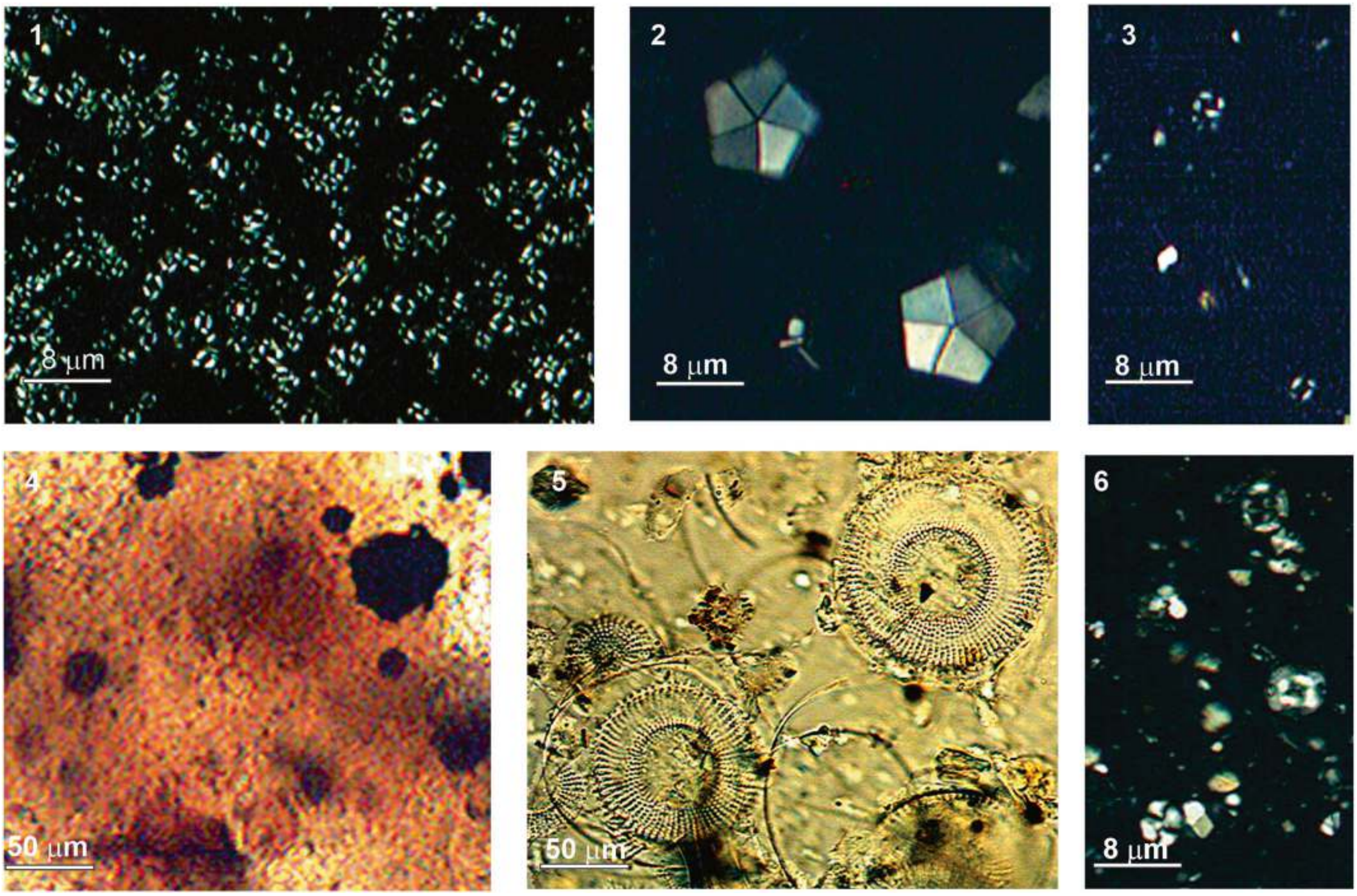

Plate 1. Calcareous nannoplankton microphotographs at LM (light microscope), N+ (crossed-nicols) (1–3 and 6); 1 - Bloom of *Emiliania huxleyi* (Lohmann 1902) Hay & Mohler, in Hay et al. (1967), Core 1GC1, interval 0–4 cm, Unit 1 – Cocccolith Mud. 2 - Few specimens of *E. huxleyi* (Lohmann 1902) Hay & Mohler, in Hay et al. (1967) and in the center *Braarudosphaera bigelowii* (Gran & Braarud 1935) Deflandre, 1947, Core 3GC1, interval 20–24 cm, Unit 2 – Sapropel Mud upper part; 3 - Few specimens of *E. huxleyi* (Lohmann 1902) Hay & Mohler, in (Hay et al. (1967), Core 3GC1, interval 40–44 cm, Unit 2 – lower part of the Sapropel Mud; 6 - Reworked Cretaceous and Tertiary taxa in Unit 3 – Lacustrine Lutite, Core 1GC1, interval 420–424 cm. 4 – Organic matter of Unit 2 Sapropel Mud, Core 3GC1, interval 40–44 cm; 5 - Centric diatoms identified in the Core 1GC1, upper part of Unit 3, Lacustrine Lutite, interval 100–104 cm, LM (light microscope), NII (polarized light).

units (youngest first):

(i) Unit 1 - The Coccolith Mud, composed of light gray silty clays, interbedded with mm-thick coccolith laminae. The thickness of this unit averages 20 cm, reaching 28 cm in 4GC1, at 840.3 m water depth and shifting to 18 cm in 5GC1 at 620 m and respectively 8GC1, at 1315 m water depths. The coccolith laminae are around 0.4 mm-thick.

(ii) Unit 2 – The Sapropel Mud, made by a fine-grained brownish-blackish mud, displaying a variable thickness in the study area. The maximum of 96 cm was observed in the 7GC1, at 1053 m water depth, while the minimum, 24 cm, was identified in the 8GC1 at 1315 m water depth (Fig. 3). The Sapropel Mud thickness averages 25 cm. At the base of Unit 2, millimeter-scale coccolith laminae composing a 4 cm-thick interval, are present. Two exceptions are to be noted: (i) in core 10GC1, at 940.1 m water depth, a thicker depositional interval, i.e., 25 cm, containing coccolith laminae was identified, while the whole Unit 2 is thicker (up to 55 cm) as in the other studied cores; (ii) in core 7GC1, Unit 2 is 96 cm-thick and contains two distinct depositional intervals with millimeter-scale coccolith laminae. Another feature of Unit 2 in the aforementioned core is the presence of a blackish mud at the base, rich in black specks of organic matter. Unlike the other cores, no millimeter-scale coccolith laminae occur at the base of the Unit 2 in core 7GC1.

(iii) Unit 3 – The Lacustrine Lutite, made by 120 up to 150 cm in thickness green-grayish clays, rich in black specks of organic matter. The green-grayish clays overlie a succession of red-brownish clays and muds, also rich in black specks of organic matter and showing a variable thickness, i.e., between 50 and 160 cm. Some cores contain two distinct red-brownish subunits, mainly made by clays, separated by gray-greenish clays.

Below 172 m water depth, the Units 1 and 2, the Coccolith Mud and the Sapropel Mud, are replaced by a succession composed of light gray mud and gray-greenish silty clays, with specks of black organic matter. A characteristic of this unit is the presence of cm-thick fine silty sands and coquinas, mainly made by brackish and fresh-water mollusks, which are more numerous and thicker below 160 m water depth. A dominance of shell detritus over whole shells (intact and fragments) was remarked. The oldest sediments of the analyzed cores are similar with the ones assigned to Unit 3 in deep water, but the red-brownish depositional interval present in the deep basinal setting was not encountered shallower than 160 m water depth.

4.2. *Calcareous nannoplankton*

In the shallowest studied setting, i.e., at 172 m water depth, in core 1GC1 (Figs. 1 and 2), a high abundance of *E. huxleyi* was recorded in the youngest Unit 1 - Coccolith Mud. The highest bloom is placed at the top of Unit 1, where almost 3000 specimens/mm^2 were recorded.

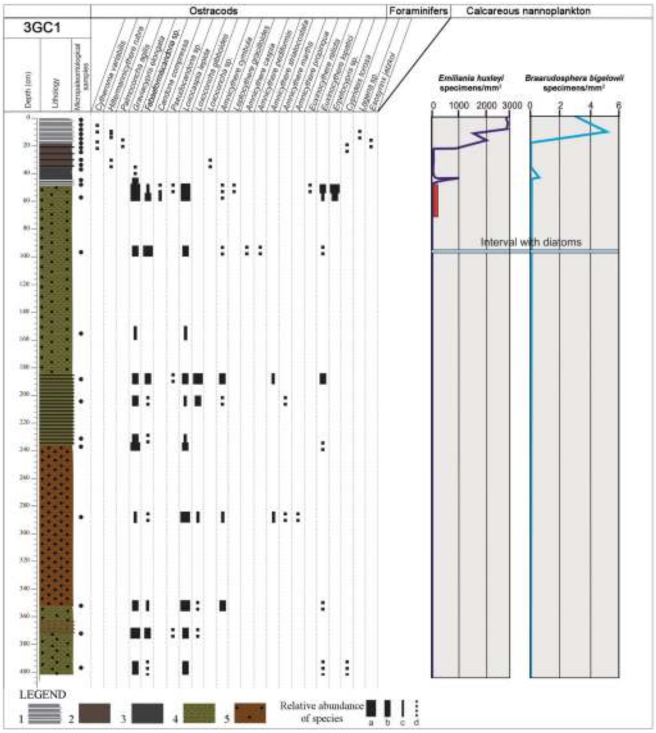

Fig. 5. Microfaunal (ostracods and foraminifers) distribution and abundance and fluctuation in abundance of calcareous nannoplankton taxa *Emiliania huxleyi* and *Braarudosphaera bigelowii* (specimens/mm^2) in Core 3GC1 (modified after Melinte-Dobrinescu et al., 2019). Relative abundance of ostracods and foraminifers: a: ≥ 20 specimens; b: 7–20 specimens; c: 4–6 specimens; d: 1–3 specimens. Red rectangle – interval of *E. huxleyi* occurrence in Unit 3. For lithology see legend in Fig. 2. (For interpretation of the references to colour in this figure legend, the reader is referred to the web version of this article.)

Braarudosphaera bigelowii, the other in situ calcareous nannoplankton species encountered, shows also high values in Unit 1 and disappears below (Fig. 4, Plate 1). The 6.6 specimens/mm^2 peak of this species is remarked in the middle part of Unit 1, interval where *E. huxleyi* abundance shifts from almost 3000 specimens/mm^2 to 2050 specimens/mm^2.

In core 3GC1, situated at a water depth of 655.7 m (Figs. 1 and 2), a similar abundance of *E. huxleyi*, as recorded in the shallow core 1GC1 was remarked in Unit 1. At the top of Unit 1 – Coccolith Mud, *E. huxleyi* abundance is high, 2970 specimens/mm^2 and decreases to 380 specimens/mm^2 at the top of the overlaying Unit 2 – Sapropel Mud (Fig. 5). A recovery, up to 1820 specimens/mm^2, was identified within Unit 2, followed by the disappearance of this species in the lower part of Unit 2. A small peak, 980 specimens/mm^2, was observed in the coccolith laminae placed at the base of Unit 2. In the oldest lithological Unit 3, along with reworked nannofossils, *E. huxleyi* is still present towards the top of this unit, with an extremely low abundance (Fig. 5, Plate 1).

The other in situ calcareous nannoplankton species, *B. bigelowii*, shows a moderate frequency in Unit 1, up to 2.1 specimens/mm^2, while below, at the boundary between units 1 and 2 increased up to 5.7 specimens/mm^2. The species shortly occur towards the base of Unit 2 and it was not encountered in Unit 3.

A particular feature was observed in Core 3GC1, where an interval of high abundance of diatoms has been observed, towards the top of Unit 3, in the gray-greenish clays (Fig. 5 and Plate 1). The diatom taxa mostly belong to the centric group.

In a deep marine setting, at 1315 m water depth, in the Core 8GC1 (Figs. 1 and 2), a high abundance of *E. huxleyi* species was recorded in Unit 1 (Fig. 6). A similar distribution pattern as observed in the other investigated cores is shown by this taxon: rapid shift from a very high abundance at the top of Unit 1 to a low one, i.e., 180 specimens/mm^2, in Unit 2. In the oldest 4.5 cm of Unit 2, a small peak of 1150 specimens/mm^2 of *E. huxleyi* was encountered. A low abundance, i.e., <4–5 specimens/mm^2, was observed towards the top of Unit 3; besides, many Mesozoic and Tertiary reworked calcareous nannoplankton taxa are present (Plate 1).

B. bigelowii is present in the whole Unit 1, with a maximum of 7.8 specimens/mm^2. The taxon decreases to very low values, i.e., below 0.3 specimens/mm^2 in Unit 2 and shows a small revival at the top of coccolith laminae placed at the base of the above-mentioned unit. Below, in Unit 3, the species vanished.

Like in the Core 3GC1, an interval rich in diatoms was observed. This interval is situated in the gray-greenish clays deposited at top of Unit 3.

4.3. *Microfaunas*

Totally, 29 ostracod species and 7 foraminiferal species were recorded in the samples from the three studied cores, i.e., 1GC1, 3GC1 and 8GC1. Based on their affinities, Mediterranean or Ponto-Caspian origin, the identified ostracod species can be split into two groups: Mediterranean type, from which 3 taxa were identified and Ponto-Caspian type that contains 26 taxa (Table 8).

In a shallow environment, in core 1GC1 at 172 m water depth, the ostracod abundance varies from 55 to 832 specimens/sample (Table 2). The most abundant species are *Hiltermannicythere rubra*, *Palmoconcha agilis*, *Graviacypris elongata*, *Loxocaspia lepida* and *Amnicythere martha*. The Mediterranean type taxa dominates the upper part of the core, i.e., interval 0–26 cm, representing around 90% of the total ostracod assemblage.

The interval 0–26 cm (that contains 5 samples) comprises also abundant foraminifers, reaching 368 specimens of *Ammonia tepida* between 15 and 21 cm. The foraminifer assemblage shows the higher diversity recorded in the studied cores, i.e., 6 species, in the interval 0–21 cm. This interval corresponds to Unit 1. Below this unit, down to 424 cm, the Mediterranean type taxa are almost completely replaced by Ponto-Caspian ones; besides, very few foraminifers are present, only between 140 cm and 158 cm in the depositional interval corresponding to Unit 3. The highest abundance and diversity recorded in this core was found at 21 cm (at the base of Unit 1) and at 153 cm and 225 cm, in the red-brownish clays and respectively the greenish ones of Unit 3 (Fig. 4). The ostracod shells are associated with juveniles or fragments of bivalves; from the top of the core down to 21 cm, mostly *Mytilus galloprovincialis* shells were recorded, while from 21 cm to 424 cm *Dreissena rostriformis* shells are present, along with gastropods and fish bones (Fig. 4 and Plate 2).

The upper part of the core 3GC1, between 0 and 18.5 cm, corresponding to Unit 1, contains a very scarce ostracod and foraminifera assemblages dominated by Mediterranean taxa, showing a low diversity (Fig. 5). Between 18.5 and 49 cm, within the Unit 2, the Sapropel Mud, only a few reworked juvenile ostracod and foraminifer taxa, fish bones and larva or juvenile stages of bivalves and gastropods were observed.

Below this interval, in the Unit 3, the Mediterranean ostracods are completely replaced by the Ponto-Caspian ones, the later showing high abundance and diversity. The assemblages of Unit 3 are dominated by taxa of the Candonidae family, such as *Graviacypris elongata*, *Fabaeformiscandona* sp. and *Candona compressa*. The Loxoconchidae family is represented by *Loxocaspia lepida*, *Loxoconcha gibboides* and rarely *Loxoconcha* sp. The representatives of the Leptocytheridae family show a higher diversity, but are less abundant, and include *Amnicythere cymbula*, *A. caspia*, *A. pediformis*, *A. striatocostata*, *A. propinqua* and *Anisochaeta martha*. The highest ostracod diversity and abundance in this core is recorded at 53 cm, at the top of Unit 3. Frequently, the ostracod shells are accompanied by juvenile ones, fragments of bivalves (*Dreissena rostriformis*), microgastropods (especially *Ecrobia* sp.) and fish bones (Fig. 5 and Plate 2).

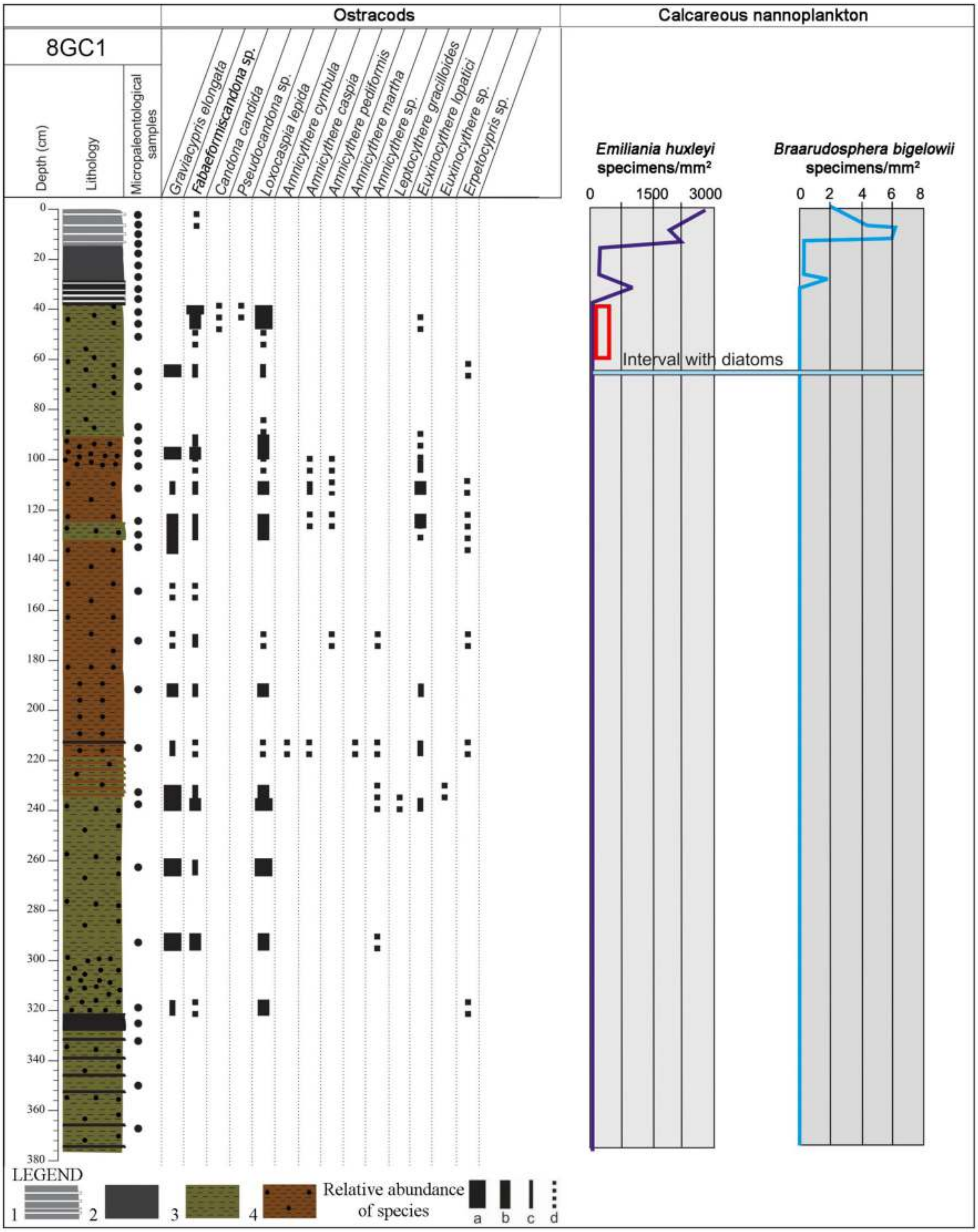

Fig. 6. Microfaunal (ostracods and foraminifers) distribution and abundance and fluctuation in abundance of calcareous nannoplankton taxa *Emiliania huxleyi* and *Braarudosphaera bigelowii* (specimens/mm^2) in Core 8GC1. Red rectangle – interval of *E. huxleyi* occurrence in Unit 3. Relative abundance of ostracods and foraminifers: a: ≥ 20 specimens; b: 7–20 specimens; c: 4–6 specimens; d: 1–3 specimens. For lithology see legend in Fig. 2. (For interpretation of the references to colour in this figure legend, the reader is referred to the web version of this article.)

In the deepest 8GC1 core (1315 m water depth), in two distinct intervals (in Unit 1, 0–14.5 cm, and Unit 2, 14.5–38.5 cm), benthic organisms, like few ostracod juveniles, larval stages of bivalves, along with gastropods and fish bones were observed. In this core no foraminifera taxa were encountered. At the top of Unit 3, the highest ostracod abundance is recorded, a bioevent similar to the one recorded in core 3GC1. The highest ostracod diversity was identified in the red-brownish clays.

The ostracods are dominated by Candonidae species, i.e., *Graviacypris elongata*, *Fabaeformiscandona* sp., *Candona candida* and *Pseudocandona* sp. The Loxoconchidae family is represented exclusively by *Loxocaspia lepida* that shows a high abundance. The Leptocytheridae family displays a low abundance, but a higher diversity; hence, *Amnicythere cymbula*, *A. caspia*, *A. pediformis*, *A. martha* and *Amnicythere* sp. are present in the assemblages. The lower part of this core, i.e., from 322 to 376.5 cm, contains no microfaunas (Fig. 6 and Plate 2).

Table 5
CaCO$_3$, TOC (Total Organic Carbon) and TOM (Total Organic Matter) values identified in the Core 1GC1.

No.	Interval (cm)	CaCO$_3$ (%)	TOC (%)	TOM (%)
1	0–5	38.094	2.669	17.870
2	5–10	33.186	3.005	18.672
3	10–15	39.205	2.672	17.238
4	15–21	19.393	0.796	6.704
5	21–26	9.449	0.532	7.092
6	26–30	7.544	0.422	8.078
7	30–35	7.643	0.385	8.899
8	35–40	7.504	0.315	8.602
9	40–45	7.589	0.164	9.350
10	45–50	9.616	0.314	7.172
11	55–60	7.649	0.255	7.852
12	65–70	12.771	0.166	8.084
13	70–75	8.628	0.166	8.216
14	75–80	54.076	0.129	8.295
15	80–85	8.506	0.202	8.104
16	90–95	10.579	0.383	8.530
17	100–105	11.665	0.352	5.326
18	110–115	9.566	0.277	4.018
19	120–125	8.324	0.639	0.919
20	130–135	8.421	0.203	3.493
21	140–145	7.903	0.508	4.974
22	145–149	8.622	0.469	5.500
23	149–153	16.548	0.254	2.548
24	153–158	13.351	0.441	3.331
25	158–163	11.730	0.182	4.090
26	170–175	10.334	0.253	0.705
27	184–189	9.675	0.399	3.466
28	189–194	12.935	0.366	2.154
29	200–205	11.767	0.400	2.960
30	210–215	12.048	0.290	3.943
31	220–225	16.894	0.144	2.576
32	225–230	7.711	0.619	3.201
33	230–235	14.319	0.181	1.946
34	250–255	15.222	0.327	3.815
35	270–275	15.827	0.180	2.369
36	290–295	13.658	0.290	2.933
37	316–321	12.554	0.396	3.386
38	335–340	13.793	0.072	2.503
39	355–360	12.360	0.252	2.601
40	380–385	12.513	0.144	2.101
41	400–405	13.209	0.109	2.904
42	420–424	13.316	0.291	2.588

4.4. Geochemistry

In general, low values of TOC (Total Organic Carbon), between 0.2% and 0.9%, has been observed in the studied cores, in the gray-green and red-brownish clays of the Unit 3 – Lacustrine Lutite. A significant sharp increase of TOC values, up to 7%, is present from the base of Unit 2 – Sapropel Mud, which is followed by a progressive decrease towards 3% up to the top of Unit 1 – Coccolith Mud (Figs. 8 and 9; Tables 3 and 4). The increase of TOC in a shallow setting (i.e., 172 m water depth - Core 1GC1), where Unit 2 is absent, starts from the base of Unit 1, the values showing small modifications, i.e., between 2.6 and 3% values (Fig. 7 and Table 2), which are slightly lower than those recorded in the coccolith laminae of Unit 1 in a deep marine environment.

The fluctuation pattern of TOM (Total Organic Matter) follows in general the trend showed by the TOC, with low values in Unit 3 and pronounced increase from the base of Unit 2 or, where Unit 2 is absent, from the base of Unit 1. The maximum, between 24 and 32% is reached at the base of Unit 2, representing an increase of 8 times compared with the underlying Unit 3. Upwards, in Unit 2, TOM values progressively shift to the top of Unit 1, at 8–10% (Fig. 7 and Tables 5–7).

The CaCO$_3$ content is low in Unit 3, up to 15%, and shows a significant increase up to 55% towards the top of the aforementioned lithological unit (Figs. 5–7). Upwards, CaCO$_3$ shifts again to lower values, i.e., <2 0%, in Unit 2 and rises again to values between 50 and 55% in Unit 1 (Fig. 7).

Table 6
CaCO$_3$, TOC (Total Organic Carbon) and TOM (Total Organic Matter) values identified in the Core 3GC1.

No.	Interval (cm)	CaCO3 (%)	TOC (%)	TOM (%)
1	0–6	50.054	2.870	10.941
2	12–18	51.708	2.972	15.179
3	18–24	26.894	3.778	13.101
4	18–24	12.055	3.758	12.747
5	24–30	12.136	5.519	17.117
6	30–36	9.758	5.595	18.300
7	36–42	11.067	7.026	27.310
8	42–48	17.439	7.140	25.886
9	48–53	52.943	0.831	6.050
10	53–58	52.916	0.748	5.391
11	65–70	53.267	0.570	4.462
12	85–90	27.180	0.862	4.535
13	95–100	24.276	0.497	3.747
14	110–115	46.279	0.902	4.738
15	125–130	28.526	0.785	5.701
16	140–145	15.942	0.709	5.076
17	155–160	11.189	0.571	7.301
18	170–175	12.793	0.498	3.793
19	185–190	6.780	0.309	2.168
20	190–195	5.453	0.420	2.565
21	200–205	5.806	0.492	3.487
22	210–215	5.884	0.461	4.477
23	220–225	5.623	0.536	2.597
24	230–235	8.584	0.351	2.754
25	235–240	5.573	0.311	2.440
26	250–255	5.642	0.346	2.618
27	265–270	6.003	0.312	3.140
28	285–290	6.348	0.237	3.002
29	305–310	8.280	0.365	3.735
30	325–330	6.329	0.397	2.163
31	348–353	7.220	0.294	3.153
32	353–358	9.112	0.324	2.977
33	370–375	7.379	0.328	3.052
34	385–390	8.670	0.343	4.195
35	396–401	9.150	0.201	4.242

Table 7
CaCO$_3$, TOC (Total Organic Carbon) and TOM (Total Organic Matter) values identified in the Core 8GC1.

No.	Interval (cm)	CaCO3 (%)	TOC (%)	TOM (%)
1	0–3	51.557	3.237	8.752
2	9–14.5	48.009	3.753	9.774
3	14.5–20	10.181	5.802	18.566
4	20–25	11.471	6.825	14.396
5	30–35	8.256	7.138	32.733
6	35–38	9.511	7.291	29.190
7	38–43	52.644	0.678	3.409
8	48–53	36.367	0.965	4.208
9	71–76	7.143	0.775	2.761
10	90–95	5.082	0.373	2.249
11	95–100	4.712	0.427	3.104
12	100–105	4.977	0.458	3.534
13	110–115	4.216	0.534	3.515
14	122–127	4.743	0.357	3.135
15	127–132	7.832	0.424	4.627
16	132–137	4.769	0.249	2.863
17	151–156	6.659	0.669	3.633
18	170–175	5.335	0.391	3.748
19	213–218	10.148	1.059	5.215
20	230–235	5.579	0.390	2.974
21	235–240	9.062	0.563	3.809
22	260–265	9.751	0.251	4.755
23	290–295	8.080	0.287	3.250
24	317–322	8.780	0.670	2.317
25	322–328	0.360	0.537	3.312
26	330–335	1.150	0.577	0.635
27	365–370	0.530	0.674	1.140

Table 8
Ecological affinity of the ostracods observed in the Core 1GC1.

Ostracod species	Faunal type	Ecological affinity
Hiltermannicythere rubra	Mediterranean	Mesohaline
Palmoconcha agilis	Mediterranean	Polyhaline
Cytheroma variabilis	Mediterranean	Polyhaline
Graviacypris elongata	Ponto-Caspian	Oligohaline
Fabaeformiscandona sp.	Ponto-Caspian	Oligohaline
Candona neglecta	Ponto-Caspian	Oligohaline
Pseudocandona sp.	Ponto-Caspian	Oligohaline
Candona sp.	Ponto-Caspian	Oligohaline
Loxoconcha lepida	Ponto-Caspian	Oligohaline
Loxoconcha gibboides	Ponto-Caspian	Oligohaline
Loxoconcha sp.	Ponto-Caspian	Oligohaline
Amnicythere martha	Ponto-Caspian	Mesohaline
Amnicythere pediformis	Ponto-Caspian	Oligohaline to mesohaline
Amnicythere caspia	Ponto-Caspian	Oligohaline
Amnicythere propinqua	Ponto-Caspian	Oligohaline
Amnicythere striatocostata	Ponto-Caspian	Oligohaline to mesohaline
Amnicythere bendovanica	Ponto-Caspian	Mesohaline
Amnicythere longa	Ponto-Caspian	Mesohaline
Euxinocythere relicta	Ponto-Caspian	Oligohaline to mesohaline
Euxinocythere lopatici	Ponto-Caspian	Mesohaline
Ilyocypris bradyi	Ponto-Caspian	Oligohaline

5. Discussion

5.1. Preconnection phase of the Black Sea

The oldest intercepted Unit 3 – The Lacustrine Lutite, sedimented during the Neoeuxine Lake stage, is present in all studied cores. It contains red-brownish clays (= brown muds of Major et al., 2002), which extends all over the western and central Black Sea basin (Fig. 8), from the Kerch Strait to the Bosporus Strait (Yanchilina et al., 2019). It is believed that the red clay origin is linked to the massive meltwater discharge brought from the Eurasian Ice Sheet by the Dnieper and Volga rivers, the later overflowing into the Caspian Sea and throughout the Manych Depression in the N Black Sea (Major et al., 2002, 2006; Bahr et al., 2005). This source is also argued by data coming from clay mineralogy, which reveals a similar composition of the red clay illite in the terraces of the lower Volga basin with those deposited in NW and central parts of the Black Sea (Major et al., 2002; Tudryn et al., 2016).

The red-brownish depositional intervals, occurring in Unit 3, were observed in all cores located between 166.7 and 1315 m water depths. In the shallowest cores 14GC1 and 11GC1 at 141.1 and 160.9 m water depths, they are not present. The significant difference in the red-brownish clay thickness (between 50 and 160 cm) is possibly due to the local paleogeographic setting.

Martinez-Lamas et al. (2020) reported fine laminations in the gray-greenish clays of Unit 3, assuming that they represent hyperpycnal floods from the Danube River. Similarly, fine laminations were described by Soulet et al. (2010) in the red brown clays and silts of the core MD04–2790, possibly linked to the meltwater annual release. In the studied cores, we found lamination both in the gray-greenish clays and the red ones of Unit 3 (Figs. 2 and 3), at various intervals and showing a variable thickness, from 2 to 3 mm up to 1.5 cm. Presumably, they reflect meltwater pulses, linked to climate changes, including more humid intervals and consequently higher denudation from land.

Some authors (Popescu et al., 2001; Lericolais et al., 2013; Constantinescu et al., 2015) reported fining-upward Bouma sequences in the red-brownish intervals, which were interpreted as episodic turbidites. This is the case of the red-brownish repetitive layers identified by us in some cores located on the canyon sides, at a water depth below 600 m, but this hypothesis needs to be further tested based on various proxies, including detailed assignment of absolute ages.

The red-brownish clays of Unit 3 found in the Core 2GC1 (166.7 m water depth) extend from 15,490 y BP, the top being younger than 13,999 y BP, according Nagavciuc et al., 2021 (Fig. 9). Based on the given data, the sedimentation of the red-brownish interval is situated from the upper part of HS1 (between 18,000 and 14,700 y BP) up to the lower part of the warmer period BA (Bølling–Allerød), placed from 14,700 and 12, 650 y BP (Lericolais et al., 2009; Soulet et al., 2013; Constantinescu et al., 2015; Yanchilina et al., 2017). Previous works indicate that the red-brownish interval is restricted to HS1 (Knutz et al., 2007; Toucanne et al., 2015). For instance, Major et al. (2002) and Bahr et al. (2005) dated the base of the red-brownish interval at ~16,400 y BP; a similar age, i.e., 16,350 y BP, was found by Briceag et al. (2019) in NW Black Sea. The later authors noted that the top of red-brownish clays, encountered in the Core 09 SG 13 (200 m water depth) is slightly above 15,150 y BP, below the boundary between HS1 and BA.

Based on the absolute age of Nagavciuc et al. (2021), the gray-green clay sedimentation rate of Unit 3 (Core 2GC1) is 23.5 cm/ka. In the same core, the sedimentation rate of the red-brownish clays is around 94 cm/ka. This finding is in agreement with previous published data (synthesis in Yanchilina et al., 2019), describing a higher sedimentation rate for the red-brownish clays, than the green-gray ones. For instance, at 1202 m water depth (Core GeoB 7608–1, placed nearby the Danube Canyon), the red-brownish clay sedimentation rate is around 200 cm/ka, almost twice bigger than the gray-green clays. The change is indicative for a sudden occurrence in the Black Sea basin of an important input of melt water and sediments from the Scandinavian and/or Siberian regions. This event allows proliferation of various organisms, including ostracods, which shows within the red clay depositional interval a higher abundance than in older and younger sediments.

The lacustrine sediments of Unit 3 contain almost exclusively oligohaline ostracods, showing Ponto-Caspian affinities. Towards the lower part of Core 1GC1 (during HS1), few mesohaline Ponto-Caspian ostracods are present. In the same core, at the top of Unit 3, within the red-brownish clays, the Mediterranean taxa already occur. This shallow core is the only one where this bioevent is present, while in the deeper cores it was not encountered, as the Mediterranean in origin ostracods are restricted to Units 1 and 2 (Figs. 4–6 and 11). Based on these data, we hypothesized that the ostracods of Core 1GC1 at the top of Unit 3, along with frequent benthonic foraminifers (Fig. 4), derived from local underwater landslides or erosion of marine sediment outcrops from previous sea-level high-stands. The lower part of Unit 3 in Core 1GC1 (around 21,000 y BP, according to Nagavciuc et al., 2021) has a very low diversity of ostracods. An interval (between 320-and 380 cm) barren of ostracods is present at the base of the deepest studied 8GC1 (1315 m water depth). These features, along with the presence of sandy layers (in Core 1GC1) is presumably related to the extreme cold of LGM between 19,500 and 23,500 y BP (Sanchi et al., 2014).

The common presence of cold-water *Fabaeformiscandona* spp. ostracod in Unit 3 (Figs. 5 and 6) suggests relatively low bottom water temperatures. In these cores, the highest abundance of the above-mentioned ostracods is recorded at the top of Unit 3, corresponding to the Younger Dryas cold period. Recent studies documented the occurrence of *Fabaeformiscandona* taxa in the low-temperature waters of the Siberian lakes (Konovalova, 2016). This author identified the emergence and development of *Fabaeformiscandona* taxa taking place during progressive global cooling with periodical climatic fluctuations. A similar high abundance of *Fabaeformiscandona* genus was reported by Briceag et al. (2019) in the NW Black Sea (at around 200 m water depth), linked, in their opinion, to the intervals when the Neoeuxinian lake surface was partially covered by ice.

Another ostracod showing a high frequency prior the reconnection with Mediterranean is *Cyprideis torosa*. This is an extremely cosmopolitan species, which survives in a wide salinity range, from freshwater to hypersaline, and tolerates high fluctuations in temperature, oxygen and substrate conditions (De Deckker and Lord, 2017*), indicating probably an unstable environment with temperature and salinity fluctuations.*

In the studied cores, below 600 m water depth, an interval with abundant diatoms was observed, towards the upper part of Unit 3, above the red-brownish depositional interval (Figs. 5 and 6 and Plate 1), this

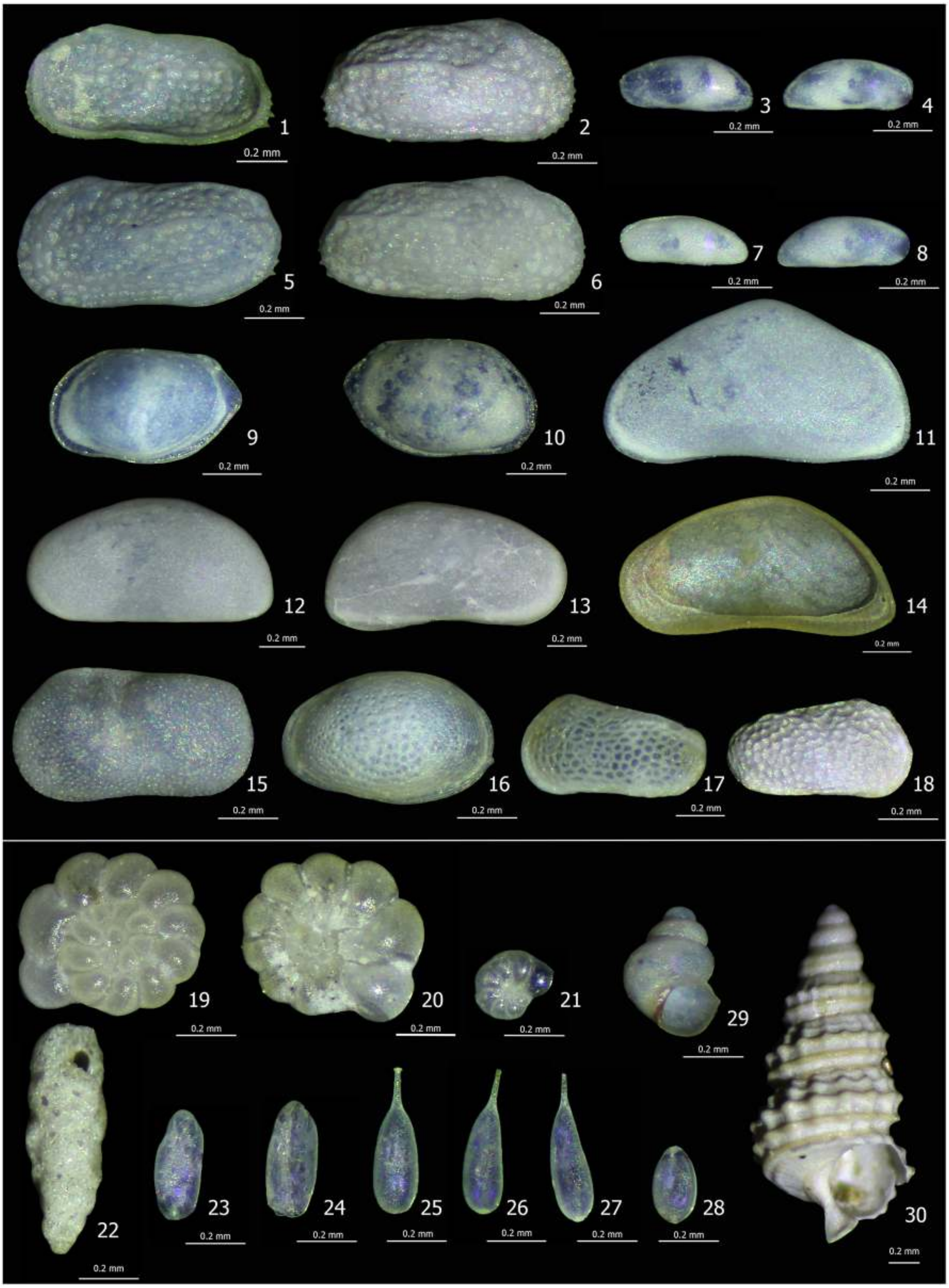

Plate 2. Identified ostracods, foraminifers and microgastropods. Photographs: 3, 7, 19, 20, 21, 23, 24, 26 and 27, Core 1GC1 interval 0–5 cm; 2, 4, 6, 8, 10, and 22, Core 1GC1, interval 5–10 cm; 1, 25, 28, 29, 30, Core 1GC1 interval 10–15 cm; 5 and 9, Core 1GC1, interval 15–21 cm; 12, 13, 16 and 18, Core 1GC1, interval 26–30 cm; 17, Core 1GC1, interval 35–40 cm; 15, Core 1GC1, interval 149–153 cm; 11, Core 8GC1, interval 38–43 cm; 14, Core 8GC1, interval 190–195 cm. All ostracod valves belong to adult individuals, external lateral views, except 14 internal lateral view; LV left valve, RV right valve. 1, 2, 5, 6: *Hiltermannicythere rubra* (Müller): 1, 5 – LV; 2, 6 – RV; 3, 4, 7, 8: *Cytheroma variabilis* Müller: 3, 7 – LV; 4, 8 – RV; 9, 10: *Palmoconcha agilis* (Ruggieri): 9 – LV; 10 – RV; 11: *Fabaeformiscandona* sp.: 11 – LV; 12: *Graviacypris elongata* (Schweyer): 12 – LV; 13, 14: *Candona* sp.: 13, 14 – RV; 15: *Ilyocypris bradyi* Sars: 15 – LV; 16: *Loxocaspia lepida* (Stepanaitys): 16 – RV; 17, 18: *Amnicythere martha* (Livental): 17 – LV; 18 – RV; 19, 20: *Ammonia tepida* (Cushman): 19 – spiral view; 20 – umbilical view; 21: *Cribroelphidium poeyanum* (d'Orbigny): 21 – spiral view; 22: *Eggerella scabra* (Williamson): 22 – side view; 23, 24: *Laryngosigma williamsoni* (Terquem): 23, 24 – side view; 25, 26, 27: *Lagena* sp.: 25, 26, 27 – side view; 28: *Fissurina lucida* (Williamson): 28 – side view; 29: *Ecrobia* sp., juvenile; 30: *Cerithidium submammillatum* (De Rayneval & Ponzi).

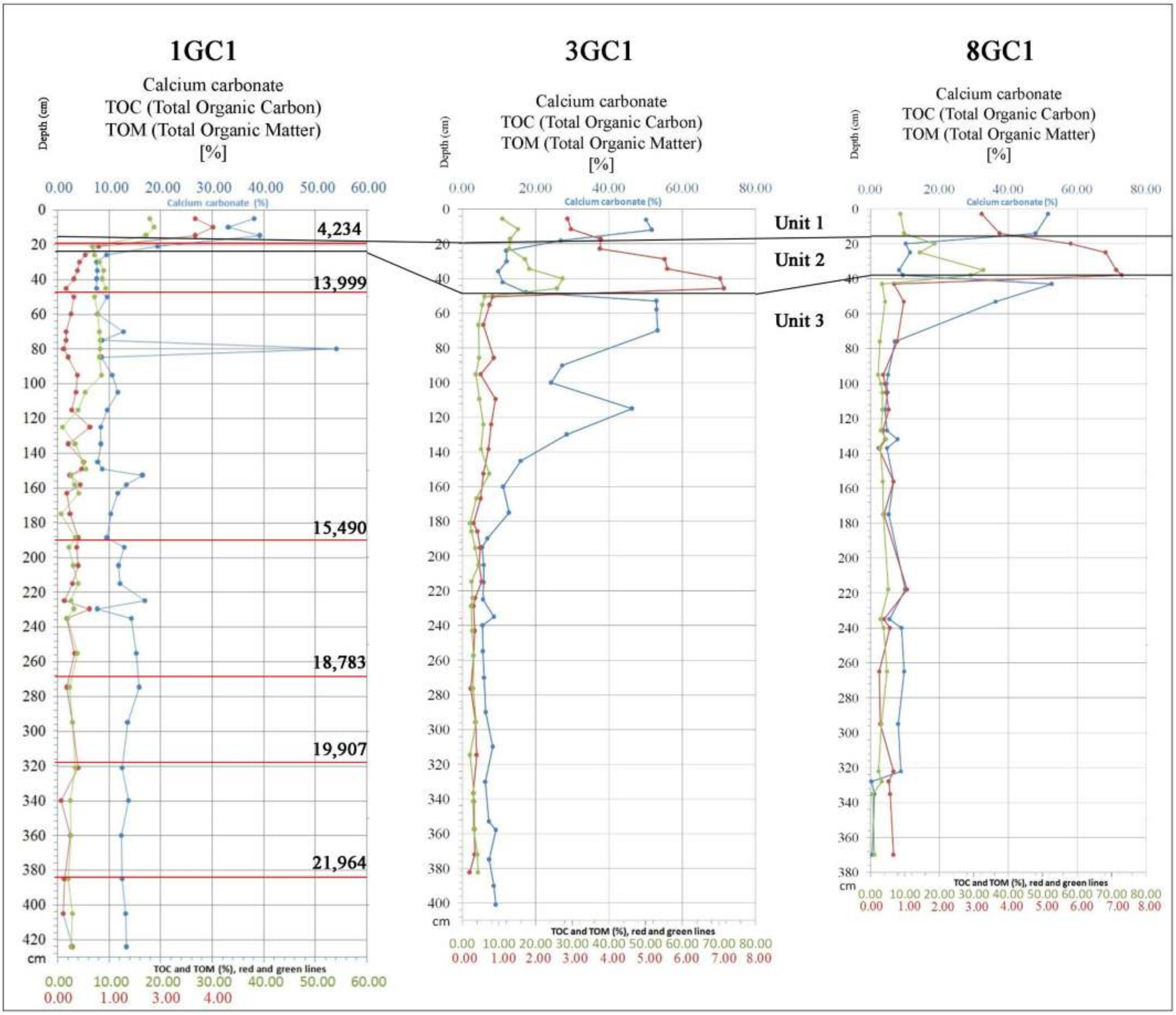

Fig. 7. Fluctuations of TOC (Total Organic Carbon), $CaCO_3$ and TOM (Total Organic Matter) identified in the studied cores 1GC1, 3GC1 and 8GC1.

being the single interval where this event was observed. The assemblages are almost monospecific and contain the taxa of the genus *Cyclostephanos*, possibly *Cyclostephanos* cf. *dubius* (Hustedt) Round in Theriot et al. (1988).

Previous studies on diatom assemblages indicate the common presence of *Cyclostephanos* (=*Stephanodiscus*) in Unit 3 (Shimkus et al., 1973; Jousé and Mukhina, 1978). In the Black Sea cores, Ryan et al. (2003) identified a high abundance of *Stephanodiscus* in the Younger Dryas. In general, the diatom genus *Cyclostephanos* and in special the species *C. dubius* is nowadays highly abundant in fresh-waters of mid to high latitudes (Bradshaw and Anderson, 2003).

Within the preconnection stage only reworked calcareous nannoplankton species were encountered. The exception is the presence of *E. huxleyi* towards the upper part of Unit 3 in the deeper studied cores, i. e., 3GC1 and 8GC1. This unexpected occurrence was firstly reported by Giunta et al. (2007), who observed a rare but regular appearance of small specimens of this taxon in the dark-gray laminae of Unit 3.

The authors advanced two hypotheses to explain this finding: (i) the coccoliths are resedimented from older marine sediments (i.e., Eemian, isotope stage 5e), but this assumption does not explain how only the smallest fragile specimens have been preserved; (ii) *E. huxleyi* derived from the passive transport by the Mediterranean waters into the Black Sea during episodic connection, constituting therefore mostly thanatocoenosis.

Possibly, the appearance of *E. huxleyi* at the top of Unit 3 indicates the increase of the salinity up to 11‰. This event might be coeval with the first invasion of Mediterranean waters, at about 9000 y. BP (Ross and Degens, 1974; Soulet et al., 2011).

Low $CaCO_3$ content is observed in Unit 3, as values of TOC and TOM. Calcium carbonate increased towards the upper part of Unit 3 above 15,490 y. BP (Figs. 7 and 10). This oldest peak is linked to the setting of the Bølling–Allerød interstadial, being reported in several sites from the NW Black Sea (Fig. 10), i.e., Briceag et al. (2019) in Core 09 SG 13, Major et al. (2002) in Core BLKS9809 and Martinez-Lamas et al. (2020).

The Bølling–Allerød $CaCO_3$ peak, along with a younger one, corresponding to the Pre-Boreal, were previously described as peaks C1 and C2 (Major et al., 2002; Ryan, 2007). They are separated by a significant $CaCO_3$ decrease of the Younger Dryas, a trend first reported by Khrischev and Georgiev (1991) in the core A96. This pattern was not identified in the shallow cores, (<200 m present-day water depth), while in

Fig. 8. Occurrence of red-brownish interval in the Unit 3 in the W Black Sea (from Yanchilina et al., 2019). Blue arrows: Meltwater gateways to the Black Sea (after Soulet et al., 2011; Yanchilina et al., 2019). Red rectangle: location of the studied cores. (For interpretation of the references to colour in this figure legend, the reader is referred to the web version of this article.)

deeper cores, i.e., 8 GC1 (1315 m water depth), only one significant $CaCO_3$ peak was observed (Fig. 7).

We found that the $CaCO_3$ Younger Dryas shift is coincident with the planktonic diatom bloom and increased abundance of the ostracod *Fabaeformiscandona* spp., bio-events reflecting an upwelling of rich in nutrients cold-waters. The $CaCO_3$ peak of Pre-Boreal times pointed out in Core 3GC1 is synchronous with rare but continuous occurrence of the nannoplankton species *E. huxleyi*.

5.2. Reconnection phase of the Black Sea with Mediterranean

The youngest Unit 1 and Unit 2 are present in all studied cores, except in the shallowest ones, above 166.7 m water depth (Fig. 2). A very thin Unit 1 (12 cm of coccolithic laminae), was observed at 172 m water depth (Core 1GC1), overlaying 8 cm-thick of dark gray mud, with TOM increased values (Fig. 7). We assume that this depositional interval represent a shallow overprint of Unit 2 – the Sapropel Mud. In this unit, Nagavciuc et al. (2021) reported an age of 4234 y BP, similar to that assigned by Jones and Gagnon (1994) and Boomer et al. (2010) in the upper part of Unit 2 (Fig. 8). This finding may indicate a development of a dysoxic regime in the NW Black Sea shelf, coeval with the anoxic setting from the deep parts of the basin.

The ostracods show an increase in abundance and diversity from the top of Unit 3, but the assemblage still contains only Ponto-Caspian taxa, while the Mediterranean species appeared in Unit 2 and the youngest Unit 1. Therefore, the 9300 y. BP (uncalibrated age) entry of Mediterranean saltwater into the Black Sea, event seen in the abrupt Sr-isotope fluctuation (Ryan et al., 2003; Major et al., 2006; Yanchilina et al., 2017; Ankindinova et al., 2019), is not reflected in the composition of the ostracod assemblage. This implies that the establishment of the bottom water salinity was not complete for allowing the survival of Mediterranean in origin ostracods into the Black Sea.

Between the upper part of Unit 3 and lower part of Unit 2, the oligohaline and mesohaline Ponto-Caspian in origin ostracods coexist, while the complete disappearance of the oligohaline taxa took place towards the upper part of the Unit 2 – Sapropel Mud. This feature reflects a brackish rather than a fresh setting of the Neoeuxinian Lake, containing benthonic species able to survive at a salinity at least >5‰. This hypothesis is supported by the absence in the Neoeuxinian Lake of the typical freshwater (lacustrine) ostracods described from various Holocene sites in Europe (Williams et al., 2018), along with our finding of *E. huxleyi* coccolith (surviving at salinity >11‰) at the top of Unit 3, in intervals where Ponto-Caspian ostracods are present. In Unit 2 a high abundance of mesohaline taxa, especially the Mediterranean in origin ostracod *Hiltermannicythere rubra*, was observed, while in Unit 1, similarly with the present-day ones, the Mediterranean polyhaline species dominated the assemblages (Fig. 11).

The highest abundance of foraminifers was observed in the shallow Core 1GC1, in Unit 1 and in the depositional interval assigned to the Sapropel Mud. In this core, the foraminifer *Ammonia tepida* shows a high abundance and a consistent occurrence from the top of Unit 3 upwards. This taxon has not been identified in 3GC1 and 8GC1 basinal cores. In general, both diversity and abundance of benthonic microfaunas (ostracods and foraminifers) diminished along with the water depth increase, a trait which may reflect the scarcity of nutrients in deep-waters.

Recent studies indicate that some benthic foraminifers, such as *Ammonia* taxa, are mostly confined to the coastal marine setting and may survive under hypoxic or full anoxic conditions (LeKieffre et al., 2017). Nowadays, a significant abundance of *Ammonia tepida* was identified in the NW Black Sea, in front of the Danube Delta, between 100 and 200 m water depth (Mureşan, 2014), while in the inner continental shelf of Bulgaria, at a salinity of 17–19‰, the species dominated the assemblages (Yanko, 1990). These observations imply that *Ammonia* taxa is highly abundant in shallow environments and show a scarce occurrence in deep ones.

As mentioned above, the coccolith *E. huxleyi* rarely occurred already towards the top of Unit 3), but its first bloom was observed at the boundary between Unit 2 and Unit 3. This feature probably mirrors an intense vertical mixing waters of the Mediterranean and Black Sea due to the spill over, enhancing the productivity at the surface water and the

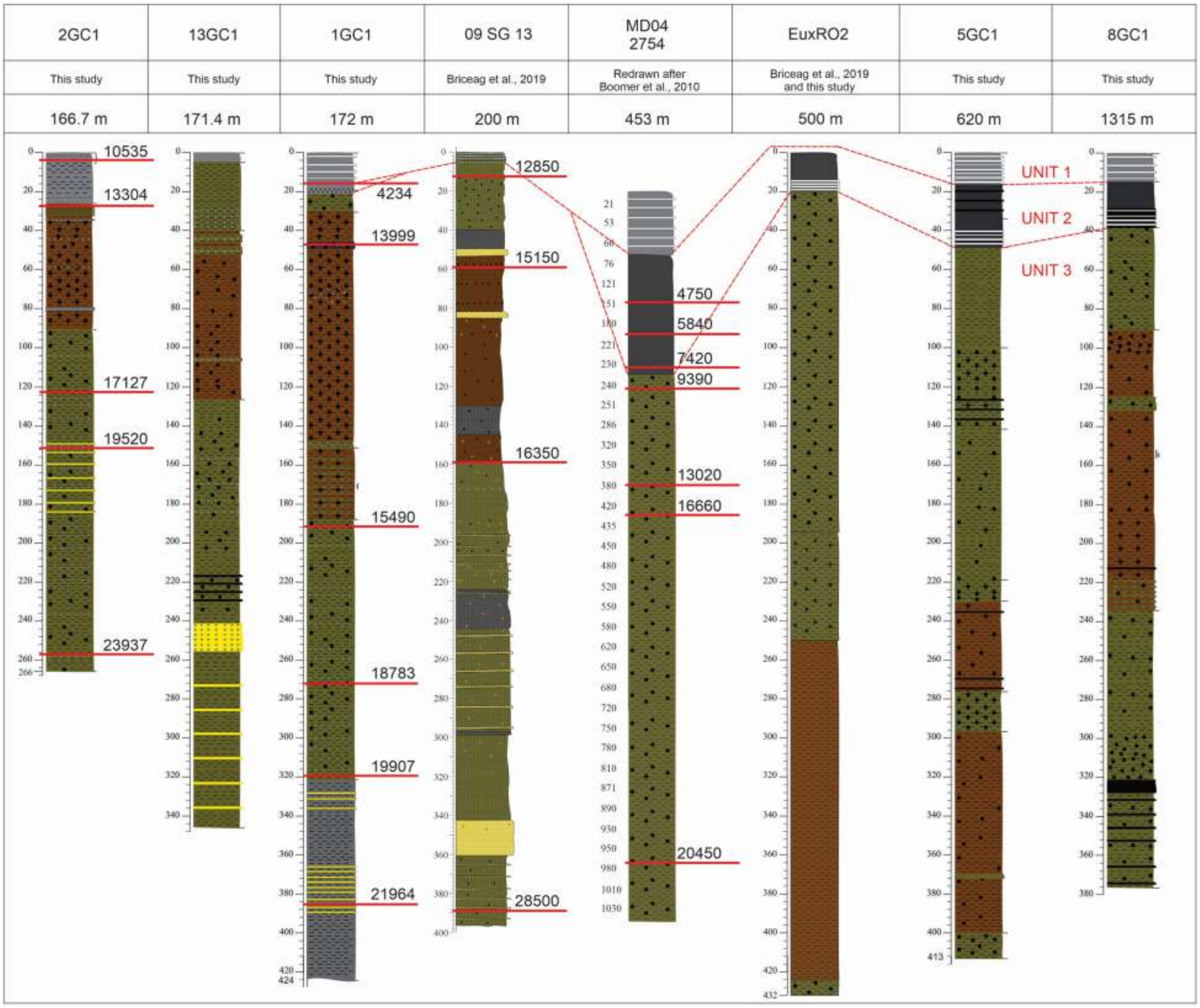

Fig. 9. Lithological and age correlation of the units encountered in various cores of the Black Sea. Data from this paper and after Boomer et al. (2010) and Briceag et al. (2019).

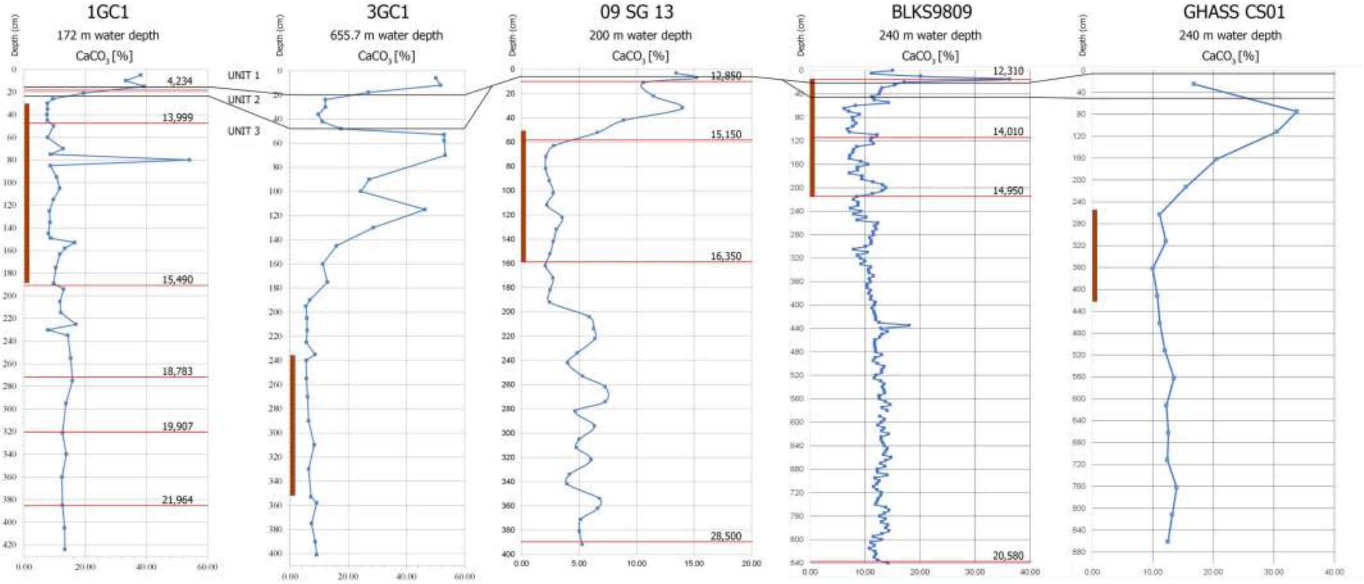

Fig. 10. Correlation of Ca CO3 fluctuations in the Upper Pleistocene-Holocene sediments of the NEW Black Sea. Cores 1GC1 and 3GC1 this study, Core 09 SG 13 after Briceag et al. (2019), Core BLKS9809 after Major et al. (2002) and Core GAS CS01 after Martinez-Lamas et al. (2020).

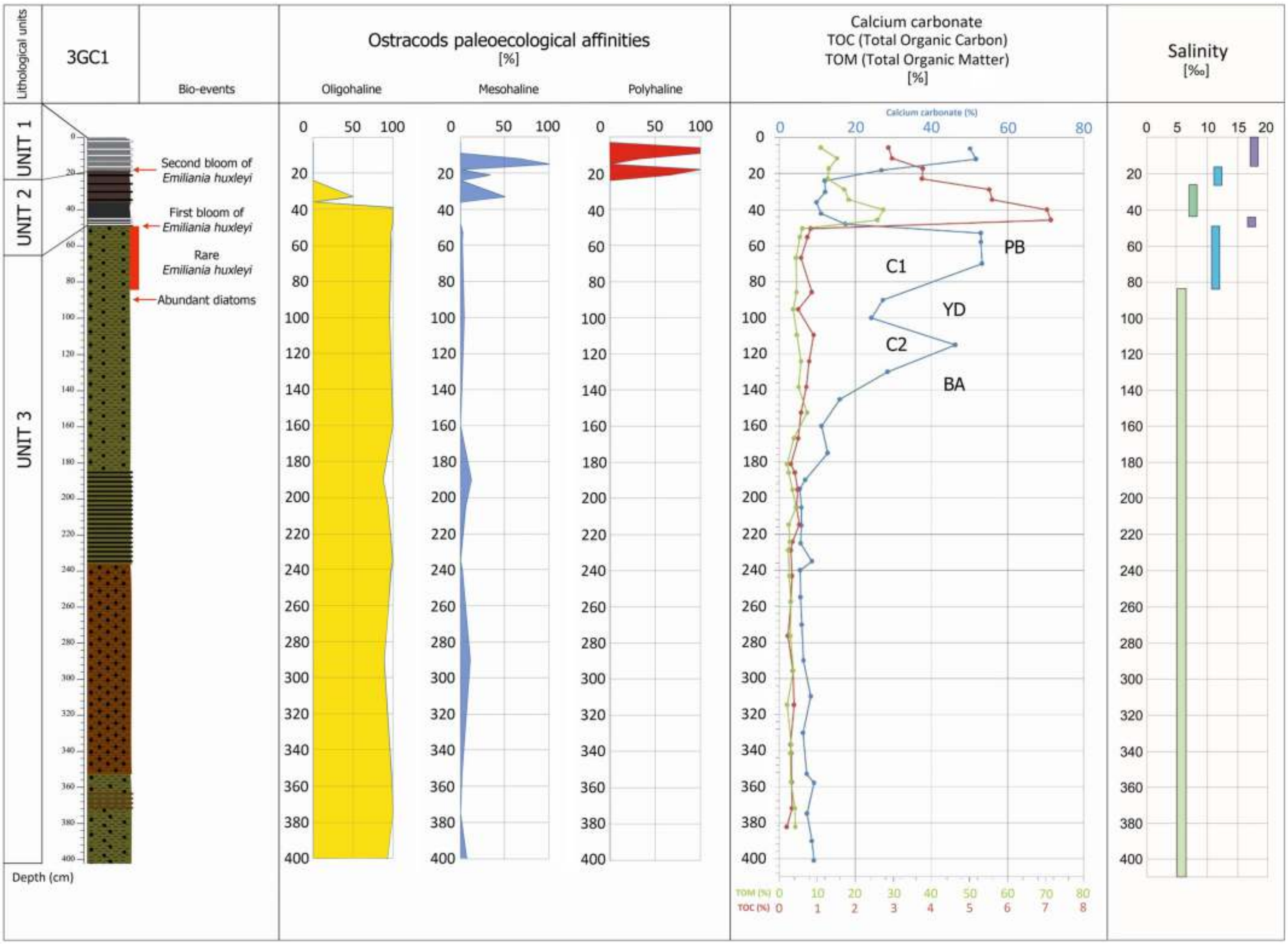

Fig. 11. Biotic, geochemical fluctuations and salinity modifications identified in Core 3GCa within the studied area during the Late Pleistocene-Holocene interval. Absolute ages after Nagavciuc et al. (2021). BA- Bølling Allerød; YD -Younger Dryas; PB-Pre-Boreal; C1 and C2 – noted after the peaks described by Major et al. (2002) and Ryan (2007) in other cores from W Black Sea.

stabilization of the salinity at a least 11‰ (Fig. 11), necessary for this species to survive (Bukry, 1974). Presently, at the NW Black Sea surface waters, in front of the Danube Delta, *E. huxleyi* was found at low salinities, i.e., 10–11‰ (Melinte-Dobrinescu and Ion, 2013). In the coccolith laminae from the base of the Sapropel, along with *E. huxleyi* occur *B. bigelowii*, indicating that the salinity was already 17‰ (value allowing *B. bigelowii* to survive – Paavola et al., 2005). Both calcareous nannoplankton species disappeared upwards, in the Sapropel Mud. This event could be interpreted as a decrease of the salinity during almost the entire depositional interval of Unit 2. However, the hypothesis that nutrients were trapped in the anoxic environment and hence not available for the plankton proliferation could not be neglected. The presence with high abundance of the two aforementioned calcareous nannoplankton species indicate the instauration of full marine condition in Unit 1, as nowadays. To note that today in the NW Black Sea, only *E. huxleyi* and *B. bigelowii* are present (Giunta et al., 2007; Melinte-Dobrinescu and Ion, 2013), while in the S Black Sea the nannoplankton assemblages are richer and diversified (Aksu et al., 2002), mirroring a higher salinity than in NW parts of the basin, which allow the proliferation of the Mediterranean species.

In Unit 2 the values of $CaCO_3$ decreased 5 times and increased again in the youngest Unit 1. This finding is in accordance with previous published works, i.e., Arthur and Dean (1998), who indicate that, in Unit 1, $CaCO_3$ values show a significant increase and it is almost entirely composed of *E. huxleyi* tests. As expected, TOC and TOM show a significant peak in the Sapropel Mud of Unit 2; above, in Unit 1 – Coccolith Mud, they decrease but not so significantly to reach the low values recorded in Unit 3. Notably, TOC and TOM start to increase slightly prior the Sapropel Mud, possibly linked to an early flux of carbon to the sea floor leading to a high productivity.

6. Conclusions

Based on the study of 13 cores collected from the NW Black Sea, we have pointed out biotical and geochemical fluctuations in shallow and deep-water settings. The Late Holocene lithological units 1 - Coccolith Mud and 2 - Sapropel Mud are well developed in deep-waters and vanished in a shallower setting. They are replaced by a “Shallow Unit”, as firstly observed in the NW Black Sea inner shelf by Giunta et al. (2007), which contains a structureless succession of gray-green clay and sands, along with frequent coquinas, devoid of any Holocene calcareous nannoplankton taxa. These features, i.e., the absence of coccoliths and common presence of sandy layers, was not recognized in the southern part of the Romanian Black Sea Shelf (Oaie and Melinte-Dobrinescu, 2012), as in this area the impact of the Danube sedimentary input was lower than in the N region and the salinity was higher during Holocene times.

Taking into account that the building up of the Danube Delta edifice, including the initial split, took place between 11,700 y. BP and 7500 y. BP (Panin et al., 2004), we assume that the sedimentation of the Shallow Unit (corresponding to the deep-water Units 1 and 2) implies a significant discharge of the Danube in the NW part of the Romanian shelf those times. Additionally, the contribution of eroded bottom material could not be neglected.

The Late Pleistocene-Early Holocene glacial and meltwater sediments of Unit 3 were found to occur in all studied cores, containing sandy intercalations and shell detritus with increased frequency and thickness towards the coast. In the shallowest cores, the shell detritus prevails over the whole shells. As this is a characteristic of a region placed under the active influence of waves, we assume that the region of the paleo-Danube Delta front was a very shallow environment, i.e., littoral and partly an emerged area.

The red-brownish depositional intervals of Unit 3, with a variable lithology and high sedimentary rate, covering the upper part of Heinrich Stadial 1 and the lower part of the warmer Bølling–Allerød interval (Nagavciuc et al., 2021), disappeared in the shallow setting. At the upper part of Unit 3, the common presence of fresh-water planktonic diatoms more related to mid and high latitudes, along with high abundance of Ponto-Caspian cold-water ostracods, and a pronounced shift of $CaCO_{3,}$ point out the initiation of the cooler Younger Dryas interval. The decrease of CaCO3 is placed between two pronounced peaks, formerly assigned (Khrischev and Georgiev, 1991; Major et al., 2002; Ryan, 2007) to the Bølling–Allerød and Pre-Boreal interstadials.

The lower part of the studied cores contains very scarce ostracod assemblages, or even barren intervals (i.e., between 380 and 320 cm in Core 8GC1, 1315 m water depth), feature that might be related to the maximum LGM. If the Neoxinian lake surface was partly frozen at that time of extreme cold (as assumed by Briceag et al., 2019), the ventilation of the lake interior diminished to a level which the benthic fauna could not tolerate.

E. huxleyi is present from the top of Unit 3, indicating a rapid rise of the salinity at 10–11‰. However, the Neoeuxinian Lake was at least brackish in deeper parts (possible between 6 and 10‰). This scenario is based on the presence of some Ponto-Caspian ostracods in the same occurrence interval with *E. huxleyi* in Unit 3 and lower part of Unit 2. The complete disappearance of Ponto-Caspian ostracod took place in Unit 2, above the first occurrence of the nannoplankton species *Braarudosphaera bigelowii*, when the salinity values were >17‰.

Data availability

Datasets related to this article can be found at https://doi.org/10.17632/ch9vrw2m9f.1, an open-source online data repository hosted at Mendeley Data (Ion et al., 2021).

Declaration of Competing Interest

The authors declare that they have no known competing financial interests or personal relationships that could have appeared to influence the work reported in this paper.

Acknowledgements

This study was jointly supported by The Executive Agency for Higher Education, Research, Development and Innovation Funding (UEFISCDI) through the Project 24PCCDI/2018 uBiogas and by the Ministry of Research and Innovation Programme Nucleu, Projects No. 19 20 03 01 and 19 20 01 01. We thank to the whole crew of the research vessel *Mare Nigrum*, for support during the scientific cruises on the Black Sea. The authors thank Simona Saint Martin for constructive discussion on diatoms found in the studied cores. We also thank two anonymous reviewers for their valuable comments, which significantly improved the content of the paper.

References

Aksu, A.E., Hiscott, R.N., Yaşar, D., 1999. Oscillating Quaternary water levels of the Marmara Sea and vigorous out-low into the Aegean Sea from the Marmara Sea-Black Sea drainage corridor. Mar. Geol. 153, 275–302.

Aksu, A.E., Hiscott, R.N., Kaminski, M.A., Mudie, P.J., Gillespie, H., Abrajano, T., Yaşar, D., 2002. Last Glacial–Holocene paleoceanography of the Black Sea and Marmara Sea: stable isotopic, foraminiferal and coccolith evidence. Mar. Geol. 190, 119–149.

Ankindinova, O., Hiscott, R.N., Aksu, A.E., Grimes, V., 2019. High-resolution Sr-isotopic evolution of Black Sea water during the Holocene: implications for reconnection with the global ocean. Mar. Geol. 407, 213–228.

Arthur, A.M., Dean, W.E., 1998. Organic-matter production and preservation and evolution of anoxia in the Holocene Black Sea. Paleoceanography 13, 395–411.

Bahr, A., Lamy, F., Arz, H., Kuhlmann, H., Wefer, G., 2005. Late glacial to Holocene climate and sedimentation history in the NW Black Sea. Mar. Geol. 214 (4), 309–322.

Bahr, A., Arz, H.W., Lamy, F., Wefer, G., 2006. Late glacial to Holocene paleoenvironmental evolution of the Black Sea, reconstructed with stable oxygen isotope records obtained on ostracod shells. Earth Planet. Sci. Lett. 241, 863–875.

Boomer, I., Horne, D.J., Slipper, I.J., 2003. The use of ostracods in palaeoenvironmental studies, or what can you do with an ostracod shell? Paleontol. Soc. Pap. 9, 153–179.

Boomer, I., Guichard, F., Lericolais, G., 2010. Late Pleistocene to recent ostracod assemblages from the western Black Sea. J. Micropalaeontol. 29, 119–133.

Bradshaw, E.G., Anderson, J.N., 2003. Environmental factors that control the abundance of *Cyclostephanos dubius* (Bacillariophyceae) in Danish lakes, from seasonal to century scale. Eur. J. Phycol. 38, 265–276.

Briceag, A., Yanchilina, A., Ryan, W.B.F., Stoica, M., Melinte-Dobrinescu, M.C., 2019. Late Pleistocene to Holocene paleoenvironmental changes in the NW Black Sea. J. Quat. Sci. 34 (2), 87–100.

Bukry, D., 1974. Coccoliths as paleosalinity indicators – evidence from Black Sea. In: Degens, E.T., Ross, D.A. (Eds.), The Black Sea – Geology, Chemistry and Biologie, Memoirs of American Association of Petroleum Geologists, vol. 20, pp. 353–363.

Bukry, D., King, A.S., Horn, M.K., Manheim, F.T., 1970. Geological significance of coccoliths in fine-grained carbonate bands of postglacial Black Sea sediments. Nature 26 (5241), 156–158.

Chepalyga, A.L., 1984. Inland Sea basins. In: Velichko, A.A., Wright, H.E., Barnosky, C. W. (Eds.), Late Quaternary Environments of the Soviet Union. University of Minnesota Press, Minneapolis, pp. 229–247.

Chepalyga, A.L., Sadchicova, T.A., Leonova, N.B., Nesmeianov, S.A., Pirogov, A.N., 2004. Caspian-Black Sea water exchange along Manyche-Kerch Watergate in the Late Pleistocene. Papers from the Int. Conf. (24-27 September 2004, Volgograd-Astrakhan), Humanistica. In: "Ekologiia antropogena i sovremennosti: priroda I chelovek" Sbornik statey Mezhdunarodnoi Konferentsii (Ecology of the Anthropogene and Contemporaneity: Nature and Man), pp. 50–53 (In Russian).

Constantinescu, A.M., Toucanne, S., Dennielou, B., Jorry, S.J., Mulder, T., Lericolais, G., 2015. Evolution of the danube deep-sea fan since the last glacial maximum: New insights into Black Sea water-level fluctuations. Mar. Geol. 367, 50–68.

De Deckker, P., Lord, A., 2017. *Cyprideis torosa:* a model organism for the Ostracoda? J. Micropalaeontol. 36, 3–6.

Fedorov, P.V., 1978. Pleistotsen Ponto-Kaspiia [Pleistocene of the Ponto Caspian Region]. Trudy Geological Institute Academy Science USSR, Nauka, Moscow, 168 pp. (In Russian).

Gaudette, H.E., Flight, W.R., Toner, L., Flager, D.W., 1974. An inexpensive titration of organic carbon in recent sediments. J. Sediment. Petrol. 44 (1), 249–253.

Giosan, L., Filip, F., Constatinescu, S., 2009. Was the Black Sea catastrophically flooded in the early Holocene? Quat. Sci. Rev. 28, 1–6.

Giunta, S., Morigi, C., Negri, A., Guichard, F., Lericolais, G., 2007. Holocene biostratigraphy and paleoenvironmental changes in the Black Sea based on calcareous nannoplankton. Mar. Micropaleontol. 63, 91–110.

Goldberg, S.L., Lau, C.P.H., Mitrovica, J.X., Latychev, K., 2016. The timing of the Black Sea flood event: insights from modeling of glacial isostatic adjustment. Earth Planet. Sci. Lett. 452, 178–184.

Goncharov, V.P., 1958. New data on the Black Sea bottom relief. Dokl. Akad. Nauk USSR 121, 830–833.

Hay, W.W., Mohler, H.P., Roth, P.H., Schmidt, R.R., Boudreaux, J.E., 1967. Calcareous nannoplankton zonation of the Cenozoic of the Gulf coast and Caribbean-Antillean area, and transoceanic correlation. Trans. Gulf Coast Ass. Geol. Soc. 17, 428–480.

Hiscott, R.N., Aksu, A.E., 2002. Late Quaternary history of the Marmara Sea and Black Sea from high-resolution seismic and gravity-core studies. Mar. Geol. 190, 261–282.

Hiscott, R.N., Aksu, A.E., Mudie, P.J., Kaminski, M., Abrajano, T., Yaşar, D., Rochon, A., Dolukhanov, P.M., 2007. The Marmara Sea Gateway since 16 ky BP: non-catastrophic causes of paleoceanographic events in the Black Sea at 8.4 and 7.15 ky BP. In: Yanko-Hombach, V., Gilbert, A.S., Panin, N. (Eds.), The Black Sea Flood Question: Changes in Coastline, Climate, and HumanSettlement. Springer, Dordrecht, pp. 89–117.

Ion, G., Lericolais, G., Nouzé, H., Panin, N., Ion, E., 2002. Seismo-acoustics evidence of gases in sedimentary edifices of the paleo-Danube realm. CIESM Workshop Ser. 7, 91–95.

Ivanova, E.V., Murdmaa, I.O., Chepalyga, A.L., Cronin, T.M., Pasechnik, I.V., Levchenko, O.V., Howe, S.S., Manushkina, A.V., Platonova, E.A., 2007. Holocene sea-level oscillations and environmental changes on the eastern Black Sea shelf. Palaeogeogr. Palaeoclimatol. Palaeoecol. 246, 228–259.

Jones, G.A., Gagnon, A.R., 1994. Radiocarbon chronology of Black Sea sediments. Deep-Sea Res. I 41 (3), 531–557.

Jousé, A.P., Mukhina, V.V., 1978. Diatom units and the paleogeography of the Black Sea in the late Cenozoic (DSDP, Leg 42B). Deep Sea Drill. Proj. Initial Rep. 42 (2), 903–950.

Kaminski, M.A., Aksu, A.E., Box, M., Hiscott, R.N., Filipescu, S., Al-Salameen, M., 2002. Late Glacial to Holocene benthic foraminifera in the Marmara Sea: implications for Black Sea-Mediterranean Sea connections following the last deglaciation. Mar. Geol. 190, 165–202.

Khrischev, K., Georgiev, V., 1991. Regional washout in the Pleistocene-Holocene boundary in the Western Black Sea depression. Comptes rendues de l'Académie Bulgaire des Science 44 (9), 69–71.

Knutz, P.C., Zahn, R., Hall, I.R., 2007. Centennial-scale variability of the British Ice Sheet: Implications for climate forcing and Atlantic meridional overturning circulation during the last deglaciation. Paleoceanography 22, 1–14.

Konovalova, V.A., 2016. Representatives of the genus *Fabaeformiscandona* Krstič, 1972 (Crustacea, Ostracoda) from Quaternary deposits of Western Siberia. Rev. Micropaleontol. 59, 168–179.

LeKieffre, C., Spangenberg, J.E., Mabilleau, G., Escrig, S., Meibo, A., Geslin, E., 2017. Surviving anoxia in marine sediments: the metabolic response of ubiquitous benthic foraminifera (*Ammonia tepida*). PLoS One 12 (5), e0177604.

Lericolais, G., Popescu, I., Guichard, F., Popescu, S.-M., Manolakakis, L., 2006. Water-level fluctuations in the Black Sea since the Last Glacial Maximum. In: Yanko-Hombach, V., Gilbert, A.S., Panin, N., Dolukhanov, P.M. (Eds.), The Black Sea Flood Question: Changes in Coastline, Climate and Human Settlement. Springer, Dordrecht, pp. 4375–4452.

Lericolais, G., Bulois, C., Gillet, H., Guichard, F., 2009. High frequency sea level fluctuations recorded in the Black Sea since the LGM. Glob. Planet. Chang. 66 (1–2), 65–75.

Lericolais, G., Guichard, F., Morigi, C., Minereau, A., Popescu, I., Rădan, S., 2010. A post Younger Dryas Black Sea regression identified from sequence stratigraphy correlated to core analysis and dating. Quat. Int. 225, 195–209.

Lericolais, G., Bourget, J., Popescu, I., Jermannaud, P., Mulder, T., Jorry, S., Panin, N., 2013. Late Quaternary deep-sea sedimentation in the western Black Sea: new insights from recent coring and seismic data in the deep basin. Glob. Planet. Chang. 103, 232–247.

Major, C., Ryan, W., Lericolais, G., Hajdas, I., 2002. Constraints on Black Sea outflow to the Sea of Marmara during the last glacial-interglacial transition. Mar. Geol. 190, 19–34.

Major, C.O., Goldstein, S.L., Ryan, W.B.F., Lericolais, G., Piotrowski, A.M., Hajdas, I., 2006. The co-evolution of Black Sea level and composition through the last deglaciation and its paleoclimatic significance. Quat. Sci. Rev. 25, 2031–2047.

Marret, F., Mudie, P.J., Aksu, A.E., Hiscott, R.N., 2009. A Holocene dinocyst record of a two-step transformation of the Neoeuxinian brackish water lake into the Black Sea. Quat. Int. 197, 72–86.

Martinez-Lamas, R., Toucanne, S., Debret, M., Riboulot, V., Deloffre, J., Boissier, A., Cheron, S., Pitel, M., Bayon, G., Giosan, L., Soulet, G., 2020. Linking Danube River activity to Alpine Ice-Sheet fluctuations during the last glacial (ca. 33–17 ka BP): insights into the continental signature of Heinrich Stadials. Quat. Sci. Rev. 229, 106136.

Melinte-Dobrinescu, M., Ion, G., 2013. *Emiliania huxleyi* fluctuations and associated microalgae in superficial sediments of the Romanian Black Sea Shelf. Geo-Eco-Marina 13, 129–135.

Melinte-Dobrinescu, M., Briceag, A., Ion, G., Roman, D., Simionescu, M., 2019. Calcareous nannoplankton fluctuation, proxy for Holocene environmental changes in the Black Sea. The 19th International Multidisciplinary Scientific GeoConference SGEM 2019. Conference Proceedings 19 (1.1), 67–73.

Mertens, K.N., Bradley, L.R., Takano, Y., Mudie, P.J., Marret, F., Aksu, A.E., Hiscott, R.N., Verleye, T.J., Mousing, E.A., Smyrnova, L.L., Bagheri, S., Mansor, M., Pospelova, V., Matsuoka, K., 2012. Quantitative estimation of Holocene surface salinity variation in the Black Sea using dinoflagellate cyst process length. Quat. Sci. Rev. 39, 45–59.

Mudie, P.J., Yanko-Hombach, V., 2019. Microforaminiferal linings as proxies for paleosalinity and pollution: Danube Delta example. Micropaleontology 65 (1), 27–45.

Mudie, P.J., Yanko-Hombach, V., Kadurin, S., 2014. The black sea dating game and holocene marine transgression. Open J. Mar. Sci. 4, 1–7.

Mureşan, M., 2014. Diversity and distribution of free-living nematodes within the Pariazoic level on the Romanian Black Shelf of the Black Sea. Geo-Eco-Marina 20, 19–28.

Nagavciuc, V., Puşcaş, R.H., Cristea, G.I., Voica, C., Stelian, R., Magdaş, D.A., Turcu, I., Sava, T., Ilie, M., Ion, G., 2021. Isotopic and elemental content of deep-sea sediments from the Black Sea. Preliminary results. Anal. Lett. 54, 280–294.

Nevesskaya, L.A., 1965. Late Quaternary bivalve mollusks of the Black Sea: their systematics and ecology. Akademii Nauk SSSR Paleontol. Instit. Trydy 105, 1–390.

Nicholas, W.A., Chivas, A.R., Murray-Wallace, C.V., Fink, D., 2011. Prompt transgression and gradual salinisation of the Black Sea during the early Holocene constrained by amino acid racemization and radiocarbon dating. Quat. Sci. Rev. 30, 3769–3790.

Oaie, G., Melinte-Dobrinescu, M.C., 2012. Holocene litho- and biostratigraphy of the NW Black Sea (Romanian shelf). Quat. Int. 261, 146–155.

Olteanu, R., 1978. Ostracoda from DSDP Leg 42B. Initial Rep. Deep-Sea Drill. Proj. 42, 1017–1038.

Opreanu, P.A., 2008. Ostracode relicte Ponto-Caspice în sectorul Românesc al Mării Negre. Geo-Eco-Marina 14, 57–62.

Paavola, M., Olenin, S., Leppakoski, E., 2005. Are invasive species most successful in habitats of low native species richness across European brackish water seas? Estuar. Coast. Shelf Sci. 64, 738–750.

Panin, N., Jipa, D., 2002. Danube River Sediment Input and its Interaction with the North Western Black Sea. Estuar. Coast. Shelf Sci. 54, 551–562.

Panin, N., Ion, G., Ion, E., 2004. The Danube Delta - chronology of lobes and rates of sediment deposition. Geo-Eco-Marina 9–10, 1–5.

Popescu, I., Lericolais, G., Panin, N., Wong, H.K., Droz, L., 2001. Late Quaternary channel avulsions on the Danube Deep-Sea Fan, Black Sea. Mar. Geol. 179, 25–37.

Popescu, I., De Batist, M., Lericolais, G., Nouzé, H., Poort, J., Panin, N., Versteeg, W., Gillet, H., 2006. Multiple bottom-simulating reflections in the Black Sea: potential proxies of past climate conditions. Mar. Geol. 227, 163–176.

Reinhardt, E.G., Patterson, R.T., SchröderAdams, C.J., 1994. Geoarcheology of the ancient harbor site of Caesarea Maritima, Israel : evidence from sedimentology and paleoecology of benthic foraminifera. J. Foraminiferal Res. 24 (1), 37–48.

Riboulot, V., Ker, S., Sultan, N., Thomas, Y., Marsset, B., Scalabrin, C., Ruffine, L., Boulard, C., Ion, G., 2018. Freshwater lake to salt-water sea causing widespread hydrate dissociation in the Black Sea. Nat. Commun. 9, 117.

Ross, D.A., Degens, E.T., 1974. Recent sediments of the Black Sea. In: Degens, E.T., Ross, D.A. (Eds.), The Black Sea: Geology, Chemistry, and Biology. American Association of Petroleum Geologists, Tulsa, USA, pp. 183–199.

Ross, D.A., Degens, E.T., MacIlvaine, J., 1970. Black sea: recent sedimentary history. Science 170, 163–165.

Ruffine, L., Deusner, C., Haeckel, M., Kossel, E., Toucanne, S., Chéron, S., Bpossier, A., Schmidt, M., Donval, J.-P., Scholz, F., Guyader, V., Ker, S., Riboulot, V., 2021. Effects of postglacial seawater intrusion on sediment geochemical characteristics in the Romanian sector of the Black Sea. Mar. Pet. Geol. 123, 104746.

Ryan, W.B., 2007. Status of the Black Sea flood hypothesis. In: Yanko-Hombach, V., Gilbert, A.S., Panin, N., Dolukhanov, P.M. (Eds.), The Black Sea Flood Question: Changes in Coastline, Climate and Human Settlement. Springer, Netherlands, pp. 63–88.

Ryan, W.B.F., Pitman III, W.C., Major, C., Shimkus, K., Moskalenko, V., Jones, G.A., Dimitrov, P., Görür, N., Sakinc, M., Yüce, H., 1997. An abrupt drowning of the Black Sea shelf. Mar. Geol. 138, 119–126.

Ryan, W.B., Major, C.O., Lericolais, G., Goldstein, S.V., 2003. Catastrophic flooding of the Black Sea. Annu. Rev. Earth Planet. Sci. 31, 525–554.

Ryan, W.B.F., Yanchilina, A., Matamoros, E., et al., 2013. Massive meltwater discharge into the Black Sea Euxine Lake. Proc. 14th RCMNS Congr. 87.

Sanchi, L., Menot, G., Bard, E., 2014. Insights into continental temperatures in the northwestern Black Sea area during the last glacial period using branched tetraether lipids. Quat. Sci. Rev. 84, 98–108.

Schornikov, E.I., 1964. An experiment on the distinction of the Caspian elements of the ostracod fauna in the Azov-Black Sea basin. Zoologicheskii Zh. 43 (9), 1276–1293.

Schornikov, E.I., 2011. Ostracoda of the Caspian origin in the Azov-Black Seas basin. Joanneum Geol. Paläeontol. 11, 180–184.

Shimkus, K.M., Mukhina, V.V., Trimonis, E.S., 1973. On the role of diatoms in the late Quaternary sedimentation in the Black Sea. Oceanology 13, 882–887.

Soulet, G., Delaygue, G., Vallet-Coulomb, C., Böttcher, M.E., Sonzogni, C., Lericolais, G., Bard, E., 2010. Glacial hydrologic conditions in the Black Sea reconstructed using geochemical pore water profiles. Earth Planet. Sci. Lett. 296, 57–66.

Soulet, G., Ménot, G., Garreta, V., Rostek, V., Zaragosi, S., Lericolais, G., Bard, E., 2011. Black Sea "Lake" reservoir age evolution since the Last Glacial—hydrologic and climatic implications. Earth Planet. Sci. Lett. 308 (1–2), 245–258.

Soulet, G., Ménot, G., Bayon, G., Rostek, F., Ponzevera, E., Toucanne, S., Lericolais, G., Bard, E., 2013. Abrupt drainage cycles of the Fennoscandian Ice Sheet. Proc. Natl Acad. Sci. USA 110 (17), 6682–6687.

Stancheva, M., 1989. Taxonomy and biostratigraphy of the Pleistocene ostracods of the western Black Sea Shelf. Geol. Balc. 19, 3–39.

Strechie-Sliwinski, C., 2007. Changements environmentaux récents dans la zone de Nord-Ouest de la Mer Noire. Geo-Eco-Marina 13. Special Publication 1, 270 pp.

Tolmazin, D., 1985. Changing coastal oceanography of the Black Sea. I: Northwestern shelf. Prog. Oceanogr. 15, 217–276.

Toucanne, S., Soulet, G., Freslon, N., Silva, J.R., Dennielou, B., Zaragosi, S., Eynaud, F., Bourillet, J.-F., Bayon, G., 2015. Millennial-scale fluctuations of the European Ice Sheet at the end of the last glacial, and their potential impact on global climate. Quat. Sci. Rev. 123, 113–133.

Tudryn, A., Leroy, S.A.G., Toucanne, S., Gibert-Brunet, E., Tucholka, P., Lavrushin, Y.A., Dufaure, O., Miska, S., Bayon, G., 2016. The Ponto-Caspian basin as a final trap for southeastern Scandinavian Ice-Sheet meltwater. Quat. Sci. Rev. 148, 29–43.

Williams, L.R., Hiscott, R.N., Aksu, A.E., Bradley, L.R., Horne, D.J., Stoica, M., 2018. Holocene paleoecology and paleoceanography of the southwestern Black Sea shelf revealed by ostracod assemblages. Mar. Micropaleontol. 142, 48–66.

Yanchilina, A.G., Ryan, W.B.F., McManus, J.F., Dimitrov, P., Dimitrov, D., Slavova, K., Filipova-Marinova, M., 2017. Compilation of geophysical, geochronological, and geochemical evidence indicates a rapid Mediterranean-derived submergence of the Black Sea's shelf and subsequent substantial salinification in the early Holocene. Mar. Geol. 383, 14–34.

Yanchilina, A., Ryan, W.B.F., Kenna, T.C., McManus, J.F., 2019. Meltwater floods into the Black and Caspian Seas during Heinrich Stadial 1. Earth-Sci. Rev. 198, 10293.

Yanko, V., 1990. Stratigraphy and palaeogeography of marine Pleistocene and Holocene deposits of the Southern Seas of the USSR. Mem. Soc. Geol. Ital. 44, 167–187.

Yanko-Hombach, V., 2004. The Black Sea flood controversy in light of the geological and foraminiferal evidence. In: Yanko-Hombach, V., Görmüs, M., Ertunç, A., McGann, M., Martin, R., Jacob, J., Ishman, S. (Eds.), Program and Extended Abstracts of the Fourth International Congress on Environmental Micropalaeontology, Microbiology, and Meiobenthology, pp. 224–227, 13–18 September, Isparta, Turkey.

Yanko-Hombach, V., Yanko-Hombach, V., 2007. Controversy over Noah's Flood in the Black Sea: geological and foraminiferal evidence from the shelf. In: Gilbert, A.S., Panin, N., Dolukhanov, P.M. (Eds.), The Black Sea Flood Question: Changes in Coastline, Climate and Human Settlement. Springer, Dordrecht, pp. 149–203.

Yanko-Hombach, V., Kislov, A., 2018. Late Pleistocene-Holocene sea-level dynamics in the Caspian and Black Seas: Data synthesis and Paradoxical interpretations. Quat. Int. 465, 63–71.

Yanko-Hombach, V., Mudie, P., Kadurin, S., Larchenkov, E., 2014. Holocene marine transgression in the Black Sea: new evidence from the northwestern Black Sea shelf. Quat. Int. 345, 100–118.

Zenina, M.A., Ivanova, E.V., Bradley, L.R., Murdmaa, I.O., Schornikov, E.I., Marret, F., 2017. Origin, migration pathways, and paleoenvironmental significance of Holocene ostracod records from the northeastern Black Sea shelf. Quat. Res. 87, 49–65.